Ph.D. DISSERTATION

Rapid drug susceptibility test of *M. tuberculosis* using single cell tracking method in agarose matrix

아가로즈 내에 단일 세포 추적 방법을 이용한 결핵균의 신속한 약제 감수성 검사 기법

BY

Choi Jungil

FEBRUARY 2015

DEPARTMENT OF ELECTRICAL ENGINEERING AND
COMPUTER SCIENCE
COLLEGE OF ENGINEERING
SEOUL NATIONAL UNIVERSITY

Rapid drug susceptibility test of *M. tuberculosis* using single cell tracking method in agarose matrix

아가로즈 내에 단일 세포 추적 방법을 이용한 결핵균의 신속한 약제 감수성 검사 기법

지도교수 권 성 훈

이 논문을 공학박사 학위논문으로 제출함

2014 년 12 월

서울대학교 대학원

전기컴퓨터 공학부

최 정 일

최정일의 공학박사 학위논문을 인준함

2014 년 12 월

위 원 장 : 박 영 준

부위원장 : 권 성 훈

위 원 : 김 성 재

위 원 : 전 누 리

위 원 : 류 성 원

Abstract

In this thesis, I describe a principle and system for rapid drug susceptibility test (DST) of *M. tuberculosis* (MTB). In the test system, single cell of MTB is immobilized in the agarose matrix and culture media with TB drugs are diffused into the agarose. The response of single cell is observed by microscopy and the images were transformed by image processing program for quantification. In case of common pathogen, antibiotic susceptibility test comparable with standard method was performed in 3 ~ 4 hours. Single cell morphological analysis is developed to handle the heterogeneous responses of bacteria in the various antimicrobial condition and the system derived an AST result satisfying the FDA standard for new AST systems. In the final, DST system for MTB was developed which can determine the DST of MDT in one week by single cell tracking method. Single cell tracking method in agarose matrix is validated as a solution for tackle the global health problem of tuberculosis and antibiotic resistance.

Keywords: Tuberculosis, Antibiotic resistant, Single cell tracking, Agarose, Drug susceptibility test

Student Number: 2011-30261

Contents

Chapter 1 Introduction 1

Chapter 2 Background 3

2.1 Need of rapid drug susceptibility test 3

2.2 The conventional DST methods 5

2.3 Single cell tracking method for rapid DST 8

Chapter 3 Rapid antibiotic susceptibility testing by tracking single cell growth 10

3.1 AST process in the MAC system 11

3.1.1 AST process in the MAC system 11

3.1.2 Interface formation between the agarose-bacteria mixture and the liquid medium 14

3.1.3 Fabrication of the PDMS MAC chip 17

3.1.4 Bacteria, chemicals, and incubation conditions 18

3.2 Rapid AST in the MAC system 18

3.2.1 Diffusion of antibiotics into agarose 18

3.2.2 Bacterial fixation and tracking bacterial single cell growth by using the MAC system 20

3.2.3 Image Processing 22

3.2.4 AST with the PDMS MAC system 24

3.3 Summary 30

Chapter 4 Single-Cell Morphological Analysis 31

4.1 AST process in the Plastic MAC system 33

4.1.1 Microfluidic agarose channel (MAC) integration with a 96-well format 33

4.1.2 Diffusion characteristics in agarose within the MAC chip 39

4.2 Single-cell morphological analysis (SCMA) for rapid and accurate AST 47

4.2.1 Development of SCMA 47

4.2.2 Automated susceptibility determination based on SCMA 68

4.2.3 SCMA for determination of antimicrobial susceptibility in clinical samples 79

4.2.4 SCMA reduces AST error rates compared with the bacterial area measuring (BAM) method 83

4.2.5 Discussion 86

4.3 Summary 91

Chapter 5 Rapid DST of M. tuberculosis by single cell tracking method 92

5.1 DST process in the disk agarose culture (DAC) system 93

5.1.1 Design of a chip and its fabrication process 93

5.1.2 DST process 96

5.2 Rapid DST of *M. tuberculosis* using the DAC system 98

5.2.1 A 3D culture formation chip for the DST of MTB 98

5.2.2 Diffusion characteristics in the DAC chip 99

5.2.3 Rapid DST using single cell tracking in the DAC system 102

5.2.4 Discussion 107

5.3 Summary 109

Chapter 6 Conclusions and Future Works １１０

List of Figures

Figure 2.1 Number of MDR-TB cases estimated to occur among notified pulmonary TB cases, 2012 [2]. 4

Figure 2.2 The process of DST using solid culture media. A patient's sputum is inoculated on the solid media. After 4 weeks, the colonies were identified in the positive culture media. Some colonies were inoculated on the solid media with TB drugs at critical concentrations. After 4~6 weeks, the colony size and number is examined by naked eye for DST [6]. 6

Figure 2.3 A conventional automated liquid culture system called MGIT 960. (A) The culture system can test 960 sample at the same time. The system incubate the MGIT tube and detect the fluorescent signal of the tube. When MTB grows in the tube, the oxygen is consumed which lead to increase the fluorescent signal in the tube. (B) MGIT tubes. Each tube contains culture media and detection part [7]. 7

Figure 2.4 Comparison of a DST based on single-cell tracking method with the solid media culture using naked eye detection. In solid media culture DST by naked eye measurement, the detection of colonies is not possible until the bacterial concentration reaches 10^7/ml, so DST is performed about 4 weeks. However, in single-cell tracking using a microscope, changes in MTB cells can be detected as soon as cells divide, so drug susceptibility can be determined in 4~5 days. 9

Figure 3.1 Schematic diagram and antibiotic susceptibility testing (AST) process for the microfluidic agarose channel (MAC) system. (A) The MAC chip was fabricated with PDMS and assembled with PDMS-coated glass. The chip was 20 mm × 20 mm in size. An agarose-bacteria mixture solution was injected into the center of the chip, which flowed synchronously into the six main channels. Different concentrations of antibiotic in the culture medium were supplied from the side-branched channels. Each interface between the agarose with

bacteria and antibiotic solutions was monitored by using a microscope to monitor bacterial cell growth. (B) (1) The empty channel before AST. (2) The bacteria were mixed with agarose and then injected into the main channels. (3) A sharp interface was generated due to the anchors (capillary valve), and then liquid medium with different concentrations of antibiotic was applied from six side-branched channels into the main channel. (4) Bacterial cell growth was tracked by using a microscope and a time lapse method [8]. 13

Figure 3.2 A schematic diagram of the channel structure including the capillary valve. The main purpose of the capillary valve was to prevent the agarose from bursting. By calculating the force of the surface tension, we could determine the optimum dimension of the structure in the microchannel. (Inset) The agarose-bacteria matrix formed the interface due to the capillary valve. The scale bar represents 100 μm [8]. 16

Figure 3.3 Diffusion of antibiotics into agarose. Image A was taken immediately after rhodamine B was loaded. Images B, C, and D were taken every 10 min in sequence. The dotted boxes show the imaging areas that were used to observe bacterial growth. The exposure time was 0.1 s. The scale bars represent 100 μm [8]. 19

Figure 3.4 Fixation and tracking of the growth of bacteria in the microfluidic agarose channel (MAC) system. Using time lapse images obtained with by microscopy, the growth of the bacteria was monitored. The bacteria were fixed firmly and grew well in the solidified and thin agarose matrix. Two types of cell growth occurred in the MAC system: dividing type (one red circle) and aggregative type (two blue circles). The scale bars represent 20 μm [8]. 21

Figure 3.5 Image processing. RGB images (A) were transformed into grey format images (B). The background was eliminated (C) and optimized (D). The processed images were changed into binary format images to enhance the image contrast (E). The scale bars represent 20 μm [8]. 2

3

Figure 3.6 Minimal inhibitory concentration (MIC) determination through image processing. (A) The MIC determination of gentamycin against *S. aureus* ATCC 29213. After image processing, the bacteria that occupied the area were measured and plotted on the graph for different concentrations of gentamycin according to the incubation time. The 1 μg/ml and 2 μg/ml concentrations did not permit bacterial growth, whereas the other concentrations increased bacterial growth according to the incubation time. From this data, the MIC of gentamycin against *S. aureus* ATCC 29213 was determined to be 1 μg/ml (B) The MIC determination of gentamycin against *P. aeruginosa* ATCC 27853. In the same procedure as that stated above, the MIC of gentamycin against *P. aeruginosa* ATCC 27853 was determined to be 2 μg/ml. The scale bars represent 50 μm [8]. 2 8

Figure 4.1 The rapid AST platform uses single bacterial-cell morphology tracking in microfluidic agarose channels. (A) Comparison of an AST based on single-cell morphological analysis (SCMA) with the conventional method using optical density (OD) measurements. In principle, the SCMA method reduces the AST time compared with conventional OD-based AST. In conventional AST by OD measurement, the OD value does not change until the bacterial concentration reaches 10^7/ml, so OD measurement cannot be performed for 6~8 hours [34]. However, in single-cell tracking using a microscope, changes in bacterial cells can be detected as soon as cells divide, so antibiotic susceptibility can be determined in 3~4 hours. (B) Schematic of the microfluidic agarose channel (MAC) chip integrated with a 96-well platform for high-throughput analysis. The MAC chip is composed of microfluidic channels containing bacteria in agarose, and a well to supply antibiotics and nutrients. The imaging region was the interface between the liquid medium and the microfluidic channel. The immobilized bacterial cells on bottoms of channels were

monitored for SCMA by time-lapse bright field microscopy. Detailed well dimensions and interfacing with 96-well plates are in Fig. 3.2. (C) Experimental procedure for the MAC chip. Bacterial cells were mixed with agarose and loaded into a microfluidic channel, where the cells were immobilized by gel solidification. Liquid nutrients, some spiked with antimicrobials, were then loaded into the wells. These liquid samples diffuse into the agarose through openings between the channels and the wells. Time-lapse imaging was performed in the imaging region (yellow box). Scale bar, 20 μm [35]..... 36

Figure 4.2 MAC chip. (A) The MAC chip is in a 96-well format and was made by an injection-molding process. (B) For automatic imaging, a focus mark (12 μm × 200 μm) was imprinted on the bottom of the film. Scale bar, 50 μm. (C) The schematic view of the MAC chip. The dimensions of the chip are 127.8 mm × 85.5 mm (same as conventional 96-well plate) and 8.0 mm of height. (D) The dimensions of the wells in the MAC chip. (E) The process of bonding of injection mold part [polycarbonate] and bottom film [poly(methyl methacrylate), thickness : 150 μm]. (F) Detailed view of capillary valve [35]..... 38

Figure 4.3 Diffusion characteristics of Rhodamine B in the imaging area of the MAC chip. After the loading of pure agarose, a fluorescent dye (rhodamine B, MW: 479.0 Da) was injected at various concentrations into the antimicrobial wells. The images were taken 30 minutes after the loading of the dye. (A) Schematic of the imaging region and the direction of flow. (B) Fluorescence images of the imaging region. The exposure time was set to 300 ms. Scale bars, 250 μm. (C) Fluorescence intensity as a function of distance from the antibiotic well containing Rhodamine B. (D) Long term time-lapse images of *E. faecalis.* Scale bar, 25 μm [35]. 44

Figure 4.4 Time-lapse images of bacteria at the different locations in the MAC chip. (A) The six different imaging regions. (B) The number of bacteria according to the each region. (C) Time-lapse images of *E. coli*

ATCC with gentamicin at the different locations. In regions 1–4, near the antibiotic well, the responses of the bacteria were identical. In regions 5 and 6, the bacteria divided regardless of antibiotic concentration. Scale bar, 25 μm [35]. 45

Figure 4.5 MIC determination analyzing bacterial number and size with *P. aeruginosa* ATCC 27853. (A) In the case of Gentamicin. At concentrations lower than 1.0 μg/ml, bacterial cells divided. However, at concentrations equal to or higher than 1.0 μg/ml, the bacterial cells stopped dividing. 1.0 μg/ml was determined as the MIC value and the MIC value was within the CLSI QC range (0.5-2 μg/ml). (B) In the case of ceftazidime. At lower concentration than 2 μg/ml, the bacterial cells divided. At concentrations equal to or higher than 2 μg/ml, ceftazidime induced filament formation (cell elongation), but the bacterial cells did not divide. 1.0 μg/ml was determined as the MIC value within the CLSI QC range (1-4 μg/ml). (C) In the case of imipenem. At concentration lower than 1.0 μg/ml, the bacterial cells were divided. At concentrations equal to or higher than 1.0 μg/ml, imipenem induced cell swelling, resulting in cells bursting, and bacterial cells did not divide. 1.0 μg/ml was determined as the MIC value within the CLSI QC range (1-4 μg/ml). Additional morphological data are provided in table S4. Scale bar, 25 μm [35].. 52

Figure 4.6 MIC determination analyzing bacterial number and size with *E. coli* ATCC 25922. (A) In the case of amikacin. At concentrations lower than 1.0 μg/ml, bacterial cells divided. However, at concentration equal to or higher than 1.0 μg/ml, the bacterial cells stopped growing. 1.0 μg/ml was determined as the MIC value and the MIC value was within the CLSI QC range (0.5-4.0 μg/ml). (B) In the case of piperacillin. At lower concentrations than 2.0 μg/ml, the bacterial cells were divided into two cells. At concentrations equal to or higher than 2.0 μg/ml, piperacillin induced filament formation (cell

elongation), but the bacterial cells did not divide. 2.0 μg/ml was determined as the MIC value and the MIC value was within the CLSI QC range (1.5-4.0 μg/ml). (C) In the case of imipenem. At concentration lower than 0.12 μg/ml, the bacterial cells divided. At concentrations equal to or higher than 0.12 μg/ml, imipenem induced cell swelling, resulting in cells bursting, and bacterial cells did not divide. 0.12 μg/ml was determined as the MIC value and the MIC value was within the CLSI QC range (0.06-0.25 μg/ml). Additional morphological data are in table S3. Scale bar, 50 μm [35]..... 54

Figure 4.7 MIC determination analyzing bacterial number with *S. aureus* ATCC 29213. (A) In the case of gentamicin. At concentration lower than 0.25 μg/ml, bacterial cells divided. However, at concentration equal to or higher than 0.25 μg/ml, the bacterial cells stopped growing. 1.0 μg/ml was determined as the MIC value and the MIC value was within the CLSI QC range (0.5-2 μg/ml). (B) In the case of ciprofloxacin. The bacterial cells grew fast and divided even at concentration equal to or higher 0.25 μg/ml in 2 hours, but did not divide anymore in 4 hours; whereas bacteria cells continually divided at concentrations lower than 0.25 μg/ml in 4 hours. (C) In the case of clindamycin. Even at concentration lower than 0.25 μg/ml, the bacterial cells divided slowly, but there was a substantial difference in the growth rate between concentrations lower than 0.12 μg/ml and concentrations equal to or higher 0.12 μg/ml. The MIC was determined as 0.12 μg/ml by comparing the relative cell growth. Scale bar, 50 μm [35]. 56

Figure 4.8 MIC determination analyzing bacterial number with *E. faecalis* ATCC 29212. (A) In the cases of vancomycin. (B) In the cases of levofloxacin. In the case of levofloxacin, the bacterial cells grew fast and divided even at concentration equal to or higher 1.0 μg/ml in 2 hours, but did not divided anymore in 4 hours, whereas bacteria cells continually divided at concentration lower than 1.0 μg/ml in 4 hours.

(C) In the case of linezolid. Even at concentrations lower than 1.0 μg/ml, the bacterial cells divided slowly, but there was a difference in the growth rate between concentrations lower than 1.0 μg/ml and at concentrations equal to or higher 1.0 μg/ml. The MIC in (B) and (C) was determined by comparing the relative cell growth. Scale bar, 50 μm [35]..... 58

Figure 4.9 Morphological categorization of single cells against antibiotics. After time-lapse imaging of the single bacterial cells, their growth patterns against the antibiotics were analyzed and classified into four groups. (A) Typical division in the antibiotic-free or the antibiotic-resistant conditions, in which bacterial cells divide into two cells. (B) Typical antibiotic-susceptible conditions, in which bacteria do not grow. (C) Filamentary formation conditions for Gram-negative strains in response to β-lactam antibiotics, in which the bacterial cells show filamentary growth, but do not divide. (D) Swelling formation conditions for Gram-negative strains in response to imipenem and meropenem, in which the bacterial cells are swollen but do not divide. Cases (C) and (D) were considered to be "susceptible". (E) Co-existence of filamentary formation and dividing. (F) Co-existence of swelling formation and dividing. Cases of (E) and (F) were considered as "resistant". *For Gram-positive strains, the time-lapse images were taken at 0, 2 and 4 hrs. Scale bar, 20 μm [35]. 67

Figure 4.10 Automated image processing and data interpretation. (A) In the case of Gram-positive strains, the raw images were transformed to binary format image by several image-processing algorithms. From the processed images, the data of total area occupancy of cells (A_i) were obtained. The value of bacterial occupancy area in third and final image at 4 hours (A_3) was divided by those of first image at 0 hours (A_1) and the calculated value was compared with the first threshold value (T_1). If A_3/A_1 was larger than T_1, the case was determined as "resistant". If the value was smaller than T_1, the second thresholding

processes comparing with the second (T_2) and third (T_3) thresholds were performed to determine susceptibility. Two calculated values from A_3/A_1 and A_3/A_2 (A_2, the second image at 2 hours) were compared with T_2 and T_3, respectively. If both values were larger than T_2 and T_3, respectively, then the case was determined as "resistant". If not, it was "susceptible". (B) In the cases of Gram-negative strains, the process was same as that of the Gram-positive strain in (A) case except an additional check of abnormal growth (filamentary formation or swelling). All cases with increased area of bacterial cells compared with the threshold values (T_4, T_5 and T_6) were sent to filament and swelling checks. Total length of bacterial cells (L_3) was divided by the number of bacterial cells (F_3), and the calculated value was compared with T_7. If the value was larger than T_7—implying filamentary formation or swelling—the case was determined as "susceptible". If not larger, it was regarded as "resistant", implying a dividing case. A_1, A_2 and A_3 are the values of bacterial growth area according to incubation times (0, 2, and 4 hours for Gram-positive strains and 0, 1.5, and 3 hours for Gram-negative strains). T_1, T_2, T_3, T_4, T_5, T_6 and T_7 are the threshold values determined individually for each strain with different growth rates under various antimicrobial agent conditions. Scale bar, 20 μm [35]. 70

Figure 4.11 Automated image processing for representative Gram-positive strains. Images represent output at each step. Details of how to perform each step are provided in table S6. (A and B) Gram-positive strains: *E. faecalis* treated with tetracycline (A) and *S. aureus* treated with rifampicin (B). First step was shading compensation, followed by adaptive filtering and binary conversion, and noise elimination and borderline clearance. Data were acquired as histograms showing the number of bacteria in bins of "area" (number of pixels occupied) of a single bacterium [35]. 72

Figure 4.12 Automated image processing for representative Gram-negative

strains. Images represent output at each step. Details of how to perform each step are provided in Table 4.8 (A and B) Gram-negative strains: *P. aeruginosa* treated with ceftazidime (A) and *E. coli* treated with imipenem (B). Images were obtained and processed similar to Gram-positive bacteria with shading compensation, adaptive filtering and binary conversion, and noise elimination and borderline clearance. However, Gram-negative bacteria with filamentary formation owing to β-lactam drugs in (A) [except the penem class in (B)] also required the following steps described in table S6: closing, line detection preparation, line detection, thinning, skeletonization, and data acquisition [35]. 75

Figure 4.13 Discrepancy rates and categorical agreement rates for SCMA using clinical samples. (A) Distribution of the 189 clinical samples from SNUH and ISMH. (B and C) The SCMA AST results were compared with the clinical gold standard BMD test. Discrepancy rate and categorical (CA) agreement rates were calculated. (B) Summary of the discrepancy and CA rates. Total values were calculated with all AST results from Gram-positive and -negative cases. For BMD test: S, susceptible; I, intermediate; R, resistant. For the SCMA: mE, minor error; ME, major error; VME, very major error. TTR, time to results. (C) CA rates according to the different clinical strains in response to β-lactam and non–β-lactam antimicrobial agents. Error bars represent 95% confidence intervals determined by Wilson's binomial method. *P*-values were determined using a chi-squared test [35]..... 81

Figure 4.14 SCMA reduces AST error rates compared with the bacterial area measuring (BAM) method. Data are the AST error rates for clinical Gram-negative strains *E. coli* (n=42), *P. aeruginosa* (n=34), and *K. pneumoniae* (n=30) tested with non–β-lactam and β-lactam antimicrobial agents. The error rates were calculated by comparing AST results from each method with BMD test. *P*-values were determined using a chi-squared test [35]. 85

Figure 5.1 A) Poly(methyl methacrylate) (PMMA) chip and its top-view. B) Rapid DST based on microscopic single cell tracking in agarose matrix takes only 4 days to obtain DST results. 95

Figure 5.2 Experimental procedure. A) Empty chamber B) Loading MTB cells mixed with agarose at liquid state at 37℃ C) Loading of drug in liquid medium D) Diffusion of drug and culture media and time lapse image to detect the MTB cell growth. E) Time lapse Single cell imaging of standard strain, H37Rv in 7H9 broth media. 97

Figure 5.3 Diffusion of antibiotics into agarose. The Image A was taken immediately after rhodamine B was loaded. Images B, C, and D were taken every 10 min in sequence. The dotted boxes show the imaging areas that were used to observe bacterial growth. The exposure time was 0.1 s. The scale bars represent 0.5mm. 101

Figure 5.4 Time Lapse Images and Processed Images. A) Raw images of H37Rv in condition of rifampicin B) Processed images. In the resistant case, many colonies of MTB formed and grew in the imaging area. After image processing, the white area represent the growing MTB colonies in the images. In the susceptible cases, there was no change of the MTB grown in the images. 103

Figure 5.5 Quantification of growth dynamics in the resistant and susceptible cases. By measuring the grown areas of MTB in the images, the growth curve was plotted. In the resistant case, the area of MTB in the images were continuously increased and the areas showed on change in the susceptible case. 104

List of Tables

Table 3.1 A comparison of the minimum inhibitory concentrations between the Clinical and Laboratory Standard Institute (CLSI) method and the microfluidic agarose channel system for 3 CLSI standard strains (units: μg/ml). [a]Time: Time required to determine the MIC (h) [8]. . 29

Table 4.1 Diffusion times into the imaging region. The imaging region was 200 μm x 200 μm. 40

Table 4.2 Molecular weights of antimicrobial agents tested in the clinical AST. The antimicrobial solution was diffused into the solidified agarose containing bacteria. The molecular weight of antimicrobials is an important parameter for calculation of diffusion characteristics.. . 41

Table 4.3 Morphological characteristics of *E. coli* ATCC 25922 in response to different antimicrobial agents. Drugs were administered at a concentration equal to or higher than the MIC. The criteria for bacterial response to a given drug were applied after 3 hours. Antimicrobial susceptibility was determined using the BMD test results and the quality control ranges from CLSI. 60

Table 4.4 Morphological characteristics of *P. aeruginosa* ATCC 27853 for different antimicrobial agents. The criteria for bacterial response to a given drug is described. The criteria for bacterial response were

applied after three hours in the MAC. The antimicrobial susceptibility was determined using the BMD test results and the quality control ranges from CLSI. 61

Table 4.5 Morphological characteristics of *S. aureus* ATCC 29213 for different antimicrobial agents. The criteria for bacterial response to were applied after four hours in the MAC. The antimicrobial susceptibility was determined using the BMD test results and the quality control ranges from CLSI. RRG, relatively rapid growth; RSG, relatively slow growth. 62

Table 4.6 Morphological characteristics of *E. faecalis* ATCC 29212 for different antimicrobial agents. The criteria for bacterial response were applied after four hours in the MAC. The antimicrobial susceptibility was determined using the BMD test results and the quality control ranges from CLSI. RRG, relatively rapid growth; RSG, relatively slow growth. 63

Table 4.7 Accurate MIC determination for the four CLSI standard strains using single-cell morphological analysis (SCMA). For validation of the SCMA, four standard bacterial strains were tested against antimicrobial agents that are commonly used in clinical areas: Gram-negative *E. coli* ATCC 25922 and *P. aeruginosa* ATCC 27853 (A); Gram-positive *S. aureus* ATCC 29213 and *E. faecalis* ATCC 29212 (B). The MIC values were determined using SCMA after time-lapse imaging. The MIC values of SCMA were compared with the MIC ranges (quality control ranges) provided by CLSI. Each test was performed in triplicate unless otherwise noted with an asterisk (*, performed twice). [a] Time to result for SCMA with *S. aureus* was 6 h. [b] Time to result for SCMA with *E. faecalis* was 6 h. 64

Table 4.8 Explanation of the image-processing algorithm. Briefly, the raw images were first processed to remove noise and obtain binary-format images representing only the background and the bacterial features. Information about the bacterial cells in the images, such as area,

number, and length, was acquired by calculating the pixel information of bacterial features in the images. 76

Table 5.1 The DST results from the DAC system. H37Rv, MDR and XDR TB strains were tested with 4 primary TB drugs, isoniazid (INH), rifampicin (RFP), streptomycin (SM), and ethambutol (EMB). The testing concentrations were determined from the critical concentration of each drugs. After determination of MIC from the time lapse images, the value were examined by the break point and drug susceptibility was determined. A) MIC values of DST from DAC b) susceptibility determination using MIC data and critical concentrations of drugs .. 106

Chapter 1 Introduction

In this dissertation, I describe a rapid drug susceptibility test of *M. tuberculosis* method using single cell tracking method in agarose matrix. Tuberculosis (TB) is one of major global health problems. To make matters worse, the drug resistant TBs such as multi-drug resistant TB (MDR-TB) and extensively drug resistance TB (XDR-TB) are spreading out in the world implying that a rapid and accurate drug susceptibility test (DST) is necessary to treat the TB patients with proper drugs. However, the conventional DST methods detecting the colony formation on solid medium requires several weeks to find out the proper drugs. To reduce the time for DST, I developed a single cell tracking method in agarose. The detailed background of this thesis is described in chapter 2.

In chapter 3, a PDMS microfluidic agarose channel (MAC) chip, as pilot test of

single cell tracking method, is introduced for rapid antimicrobial susceptibility test (AST) of common pathogen such as *E. coli*, *P. aeruginosa* and *S. aureus*. From the test, the single cell tracking method is proved as a new rapid AST. However, when I expanded the system for clinical application, there were abnormal morphologies occurred which the simple area measuring method for detection of growth of bacteria could not handle.

In chapter 4, single cell morphological analysis (SCMA) to solve the morphological difference is suggested and validated. SCMA classified antibiotic responses of bacteria to multiple cases and applied different judging criteria considering both changes in cell mass and morphology.

In chapter 5, a system for rapid DST of MTB. For single cell tracking of MTB cells is described. A microfluidic chip which contains a culture chamber was fabricated for cell immobilization and drug delivery. By observing responses of MTB to a drug with single cell resolution using microscopy, we differentiated growth and non-growth of MTB under the TB drugs and their concentrations and determined drug susceptibility only in five days which is concordance with the DST results from conventional method. This rapid DST method can reduce DST time dramatically and be used for fast and accurate treatments for TB patients leading the increase of the cure rate.

Chapter 2 Background

2.1 Need of rapid drug susceptibility test

Tuberculosis is one of the three major infectious disease threatening the global health with HIV and malaria [1]. Every each year about 1% of the population in the world contract tuberculosis and 1.3 million people were killed by TB in spite of existence of anti-tuberculosis [2]. Consequentially MDR-TB and XDR-TB is gradually increasing due to poor managing the TB patients or TB suspect [3]. Recently, the first cases of totally drug resistant TB (TDR-TB) arose from India [4]. To reduce transmission of TB and improve outcomes for TB patients, a rapid and accurate treatment after DST is required. Knowing which drug is resistant among the standard first-line anti-TB agents is important to identify MDR-TB, XDR-TB and TDR-TB and to avoid the treatment of ineffective drugs.

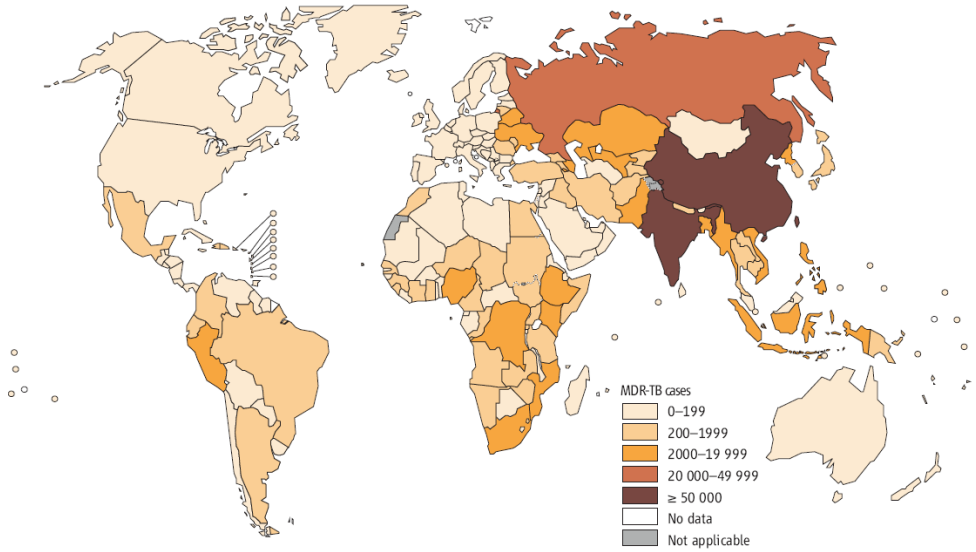

Figure 2.1 Number of MDR-TB cases estimated to occur among notified pulmonary TB cases, 2012 [2].

2.2 The conventional DST methods

The common DST methods are based on cell culture on solid and liquid media. In the solid medium culture method, *Mycobacterium tuberculosis* (MTB) is inoculated on the solid medium including an antibiotic and it is observed whether colonies is formed or not by naked eyes as in Fig. 2.2 [5]. This conventional DST method takes at least 4~6 weeks because MTB grow so slowly (cell dividing time is about 20~24 hours). In the case of liquid media, the growth of MTB is accelerated and DST time can be reduced [6]. There is a commercial DST platform using liquid media called MGIT 960 system as Fig. 2.3 [7]. The MGIT system detects a florescent signal when MTB grows and consumes oxygen and determines the drug susceptibility in one week.

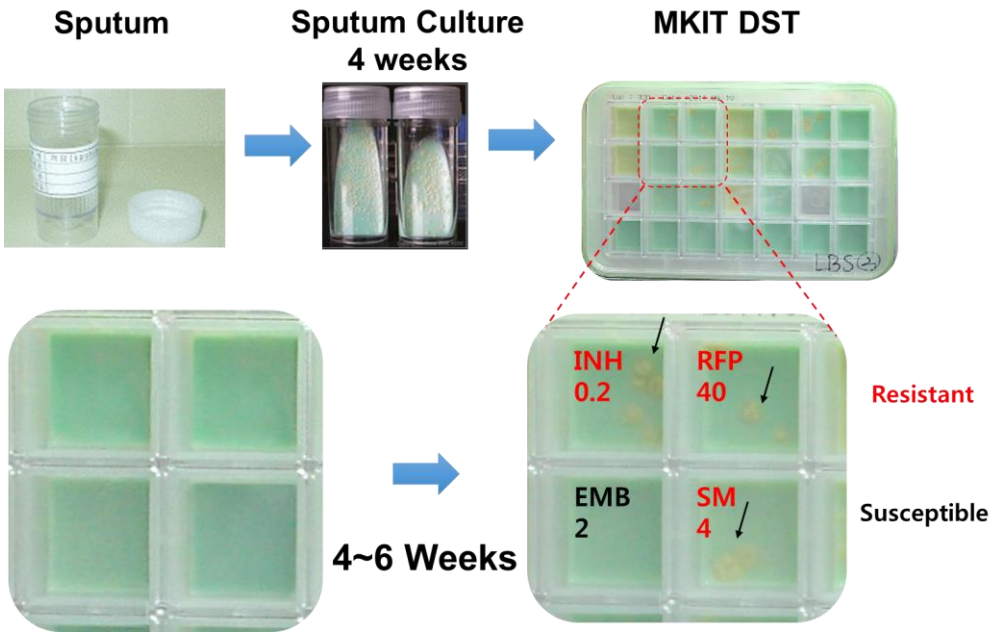

Figure 2.2 The process of DST using solid culture media. A patient's sputum is inoculated on the solid media. After 4 weeks, the colonies were identified in the positive culture media. Some colonies were inoculated on the solid media with TB drugs at critical concentrations. After 4~6 weeks, the colony size and number is examined by naked eye for DST [6].

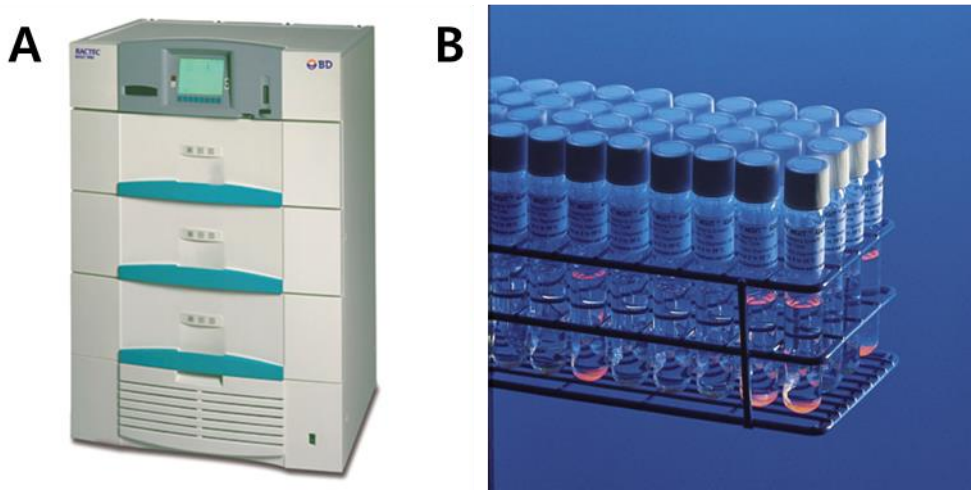

Figure 2.3 A conventional automated liquid culture system called MGIT 960. (A) The culture system can test 960 sample at the same time. The system incubate the MGIT tube and detect the fluorescent signal of the tube. When MTB grows in the tube, the oxygen is consumed which lead to increase the fluorescent signal in the tube. (B) MGIT tubes. Each tube contains culture media and detection part [7].

2.3 Single cell tracking method for rapid DST

When bacteria is inoculated in the culture media, bacteria can divide after some adaptation time. However, the current system has a limited detection sensitivity. Direct observation of the doubling of single bacterium cell in bacterial population would enable the ultimate reduction in DST time. The dividing time of MTB is about 20 ~ 24 hours and 4 ~ 5 days is enough for detection of growth of MTB (Fig. 2.4). For single cell tracking of MTB in drug condition, a new culture system is necessary which satisfies the following conditions: immobilization of single cell, sufficient delivery of culture media with drug and high resolution microscopic imaging.

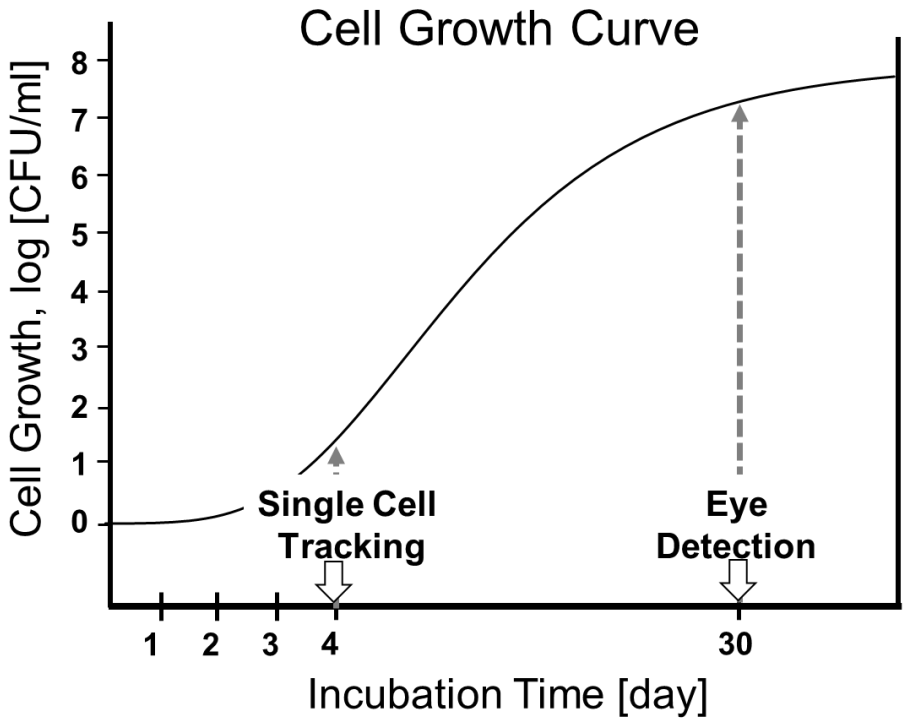

Figure 2.4 Comparison of a DST based on single-cell tracking method with the solid media culture using naked eye detection. In solid media culture DST by naked eye measurement, the detection of colonies is not possible until the bacterial concentration reaches 10^7/ml, so DST is performed about 4 weeks. However, in single-cell tracking using a microscope, changes in MTB cells can be detected as soon as cells divide, so drug susceptibility can be determined in 4~5 days.

Chapter 3 Rapid antibiotic susceptibility testing by tracking single cell growth

In this chapter, single cell tracking method is performed for rapid antimicrobial susceptibility test of common pathogen such as *E. coli*, *P. aeruginosa* and *S. aureus*. A microfluidic agarose channel (MAC) system made by polydimethylsiloxane (PDMS) was developed that reduces the AST assay time for determining MICs by single bacterial time lapse imaging. The MAC system immobilizes bacteria by using agarose in a microfluidic culture chamber so that single cell growth can be tracked by microscopy. Time lapse images of single bacterial cells under different antibiotic culture conditions were analysed by image processing to determine MICs. Three standard bacteria from the Clinical and Laboratory Standard Institute (CLSI) were tested with several kinds of antibiotics. MIC values that were well matched with those of the CLSI were obtained within only 3–4 h. We expect that the MAC system can offer rapid diagnosis of sepsis and thus, more efficient and proper medication in

the clinical setting.

3.1 AST process in the MAC system

3.1.1 AST process in the MAC system

Fig. 3.1A and 3.1B show a schematic of the MAC chip and the AST process in the MAC system, respectively. An empty channel was prepared and placed on a hot plate at 45℃ before AST (Fig. 3.1B-1). Agarose was used for delivering and fixing bacteria, as well as for permitting antibiotic diffusion and incubating the cells. 200 μl of Mueller Hinton Broth medium including approximately 5×10^8 bacteria/ml and 600 μl of 2% liquid agarose at 45℃ were mixed thoroughly by Vortexing. The agarose-bacteria mixture was placed in the six main channels using a syringe pump (KdScientific) at stable flow rate (2 ml/h). Owing to the surface tension at the anchors (capillary valve) between the main channel and the side of the channel, an agarose interface was generated (Fig. 3.1B-2). After the agarose-bacteria mixture solidified at room temperature, cation adjusted Mueller Hinton broth (CAMHB) with different concentrations of antibiotic were applied into the side branched channels by using the syringe pump at 10 μl/h, and consequently, the CAMHB medium containing the antibiotic diffused into the agarose-bacterial matrix (Fig. 3.1B-3). Since the medium with the antibiotic was supplied continuously, the

concentration of the antibiotic remained stable even at the interface between the antibiotic and the agarose matrix. Bacterial growth was monitored by using an inverted optical microscope (IX71, Olympus), and micrographs were obtained by employing a true-color CCD camera (DP71, Olympus; Fig. 3.1B-4). Images of bacterial growth were taken every hour and were analyzed by using our image processing program, which was coded in Matlab.

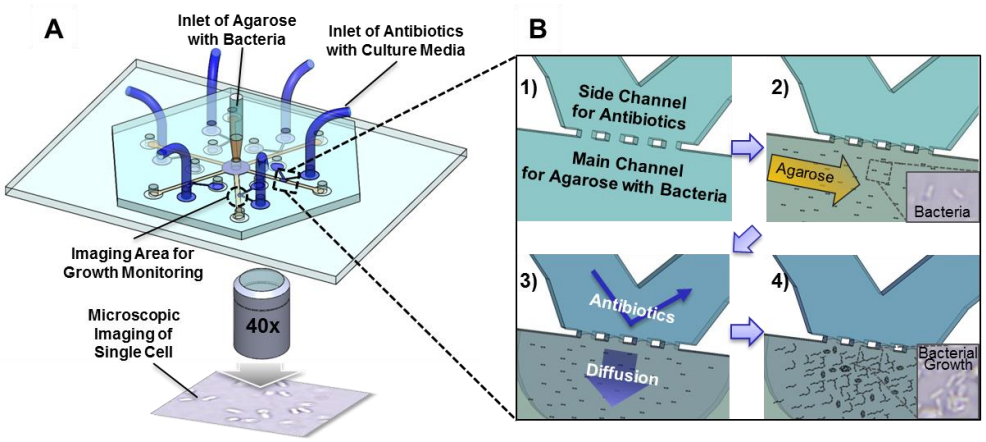

Figure 3.1 Schematic diagram and antibiotic susceptibility testing (AST) process for the microfluidic agarose channel (MAC) system. (A) The MAC chip was fabricated with PDMS and assembled with PDMS-coated glass. The chip was 20 mm × 20 mm in size. An agarose-bacteria mixture solution was injected into the center of the chip, which flowed synchronously into the six main channels. Different concentrations of antibiotic in the culture medium were supplied from the side-branched channels. Each interface between the agarose with bacteria and antibiotic solutions was monitored by using a microscope to monitor bacterial cell growth. (B) (1) The empty channel before AST. (2) The bacteria were mixed with agarose and then injected into the main channels. (3) A sharp interface was generated due to the anchors (capillary valve), and then liquid medium with different concentrations of antibiotic was applied from six side-branched channels into the main channel. (4) Bacterial cell growth was tracked by using a microscope and a time lapse method [8].

3.1.2 Interface formation between the agarose-bacteria mixture and the liquid medium

The agarose-bacteria mixture in the main channel should not burst into the side-branched channel at the interface between the bacterial agarose mixture and the liquid medium. We designed a capillary valve consisting of three anchors at the interface to block any bursting. We used a simplified Young-Laplace equation for the rectangular channel (Eqn. 2.1) to optimize the anchor size and the distance between the two anchors (Fig. 3.2) [9, 10].

$$\Delta P_{width} = P_A - P_0 = -2\gamma\left(\frac{1}{width} + \frac{1}{h}\right)$$
$$\Delta P_{gap} = P_A - P_0 = -2\gamma\left(\frac{1}{gap} + \frac{1}{h}\right) \qquad (2.1)$$
$$\Delta P_{width} - \Delta P_{gap} \geq \text{minimum threshold}$$

The fluidic contact angles at the wall were ignored in the simplified Young-Laplace equation. P_A and P_0 are the pressure of the inside and outside liquids, respectively. γ represents the surface tension, which is an intrinsic property of the material. *Width*, *gap*, and *h* are the width of the main channel, the distance between the anchors, and the height of the channel, respectively. To prevent bursting of agarose, the pressure difference should be small in the main channel but large in the side-branched channel. The surface tension is determined by agarose. In fact, the agarose slowly solidified during injection and therefore the surface tension was hard to calculate. Through several trials and errors, we optimized the channel design to

increase the pressure difference (Fig. 3.2). The width of the main channel was 500 μm, and the distance between the anchors was 45 μm. The height of the channel was 30 μm. The height of the channel was important for producing better images of bacteria that were in the channel. If the height of the channel were too thick then there would be many layers of bacteria in the focal length under the microscope. However, if the height of the channel were too thin, there would not be enough cells to determine the MIC. The 30 μm height satisfied the demands of producing a clear image and an adequate number of bacteria. Using the optimized channel design, we generated a proper interface in the channel and prevented the agarose-bacteria mixture from bursting into the side-branched channel.

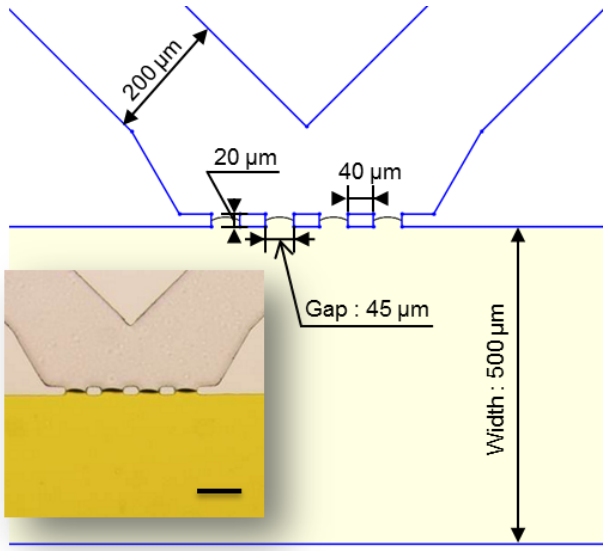

Figure 3.2 A schematic diagram of the channel structure including the capillary valve. The main purpose of the capillary valve was to prevent the agarose from bursting. By calculating the force of the surface tension, we could determine the optimum dimension of the structure in the microchannel. (Inset) The agarose-bacteria matrix formed the interface due to the capillary valve. The scale bar represents 100 µm [8].

3.1.3 Fabrication of the PDMS MAC chip

The radial shape of a MAC chip with 6 main channels and branched channels was fabricated using soft-lithography [11]. The SU-8 (Microchem Corp., Newton, MA) mold was fabricated by employing photolithography. PDMS (Sylgard 184, Dow Corning) was mixed with a curing agent (10:1 w/w) and poured into the SU-8 mold. After baking at 150℃ for 10 min, the PDMS channel was peeled off and attached to the PDMS-coated slide glass by O_2 plasma treatment (CUTE-MP, Femto Science). Fig. 3.1A shows the structure of the microfluidic channel. There were six main channels that carried one side-branched channel each. The number of channels was set at six to test six different concentrations of antibiotic according to the MIC range of the CLSI. The radial shape was chosen to cause equal fluidic resistance at each branch and thereby form interfaces between agarose and each antibiotic solution. In the middle of each main channel were micro-sized posts for blocking agarose from flowing into the side-branched channel. The sizes of the posts and the pitches were determined by mathematical calculations. The whole chip was about 20 mm long and 20 mm wide. For appropriate hydrophobicity to occur in the channel, the channel was prepared one day before AST to increase the surface tension after O_2 plasma treatment.

3.1.4 Bacteria, chemicals, and incubation conditions

To validate the MAC system, 3 standard CLSI bacteria (*E. coli* ATCC 25922, *S. aureus* ATCC 29213, and *P. aeruginosa* ATCC 27853) provided by the Seoul National University Hospital were mixed with agarose (UltraPure™ Agarose, Invitrogen) and tested to determine the MIC values of amikacin, norfloxacin, gentamycin, and tetracycline (Sigma-Aldrich). After overnight incubation of the bacteria in CAMHB medium (BBL™, BD) at 37℃ under shaking at 200 rpm, the bacteria were subcultured in fresh CAMHB medium for one hour. The number of bacteria for AST was set to 5×10^8 cells/ml, as suggested by the CLSI [12].

3.2 Rapid AST in the MAC system

3.2.1 Diffusion of antibiotics into agarose

The antibiotics reached the bacteria immobilized in the agarose matrix by diffusion. We used rhodamine B to visualize and validate the diffusion characteristics of the antibiotics. Rhodamine B has a formula weight (479.0 Da) similar to that of amikacin (585.6 Da), norfloxacin (319.3 Da), tetracycline (444.4 Da, and gentamycin (477.6 Da). Therefore, its diffusion characteristics should be similar to those of the antibiotics. A diffusion test with rhodamine B was performed to observe its diffusion into the microchannel. The diffusion test followed the AST procedure. The concentration of rhodamine B was 100 μg/ml, and the flow rate was

10 μl/h. Fig. 3.3 shows that rhodamine B diffused into the imaging area where we were able to observe bacterial cell growth for 10 min. Most of the antibiotics reached the bacteria in the imaging area within a few minutes.

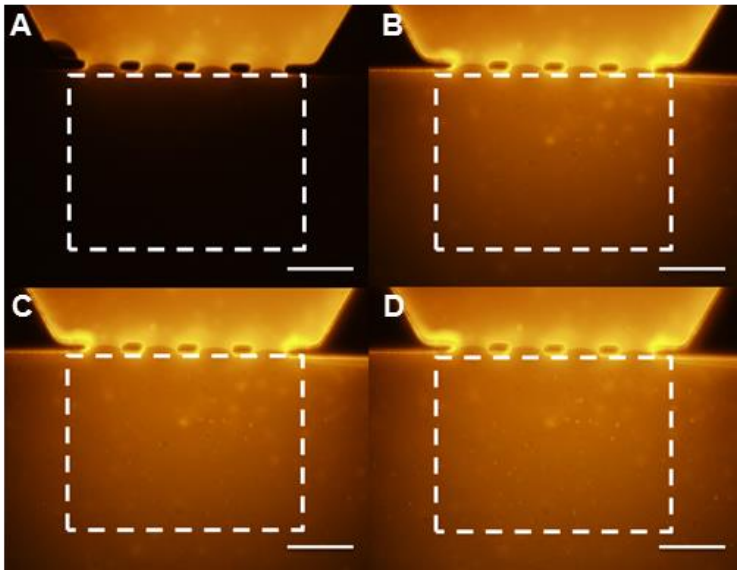

Figure 3.3 Diffusion of antibiotics into agarose. Image A was taken immediately after rhodamine B was loaded. Images B, C, and D were taken every 10 min in sequence. The dotted boxes show the imaging areas that were used to observe bacterial growth. The exposure time was 0.1 s. The scale bars represent 100 μm [8].

3.2.2 Bacterial fixation and tracking bacterial single cell growth by using the MAC system

In the MAC system, agarose was used for bacterial cell delivery and cell immobilization. Single cell growth in agarose was tracked once every hour. Agarose is a non-cytotoxic and biocompatible gelling agent, which is widely used for bacterial culturing and AST [13, 14]. In conventional AST, top agar, including the bacteria, is overlaid on an antibiotic that contains solid medium; the antibiotic then diffuses into the bacteria in the top agar [15]. Agarose is a porous material that is generally used for DNA separation by length using electrophoresis [16, 17]. Thus, most chemicals including macromolecules (DNA and proteins) and antibiotics can be freely diffused through an agarose matrix [16, 18]. In the MAC system, bacteria in CAMHB medium were mixed with 2% UltraPure^{TM} agarose (Invitrogen) at 45℃ (1:3 v/v) and immediately injected into the MAC chip (the final concentration of agarose was 1.5%). The agarose-bacteria was solidified at room temperature (25℃) for one minute. The typical number of cells that were in the imaging area was about 100 to 200. Following this, the MAC chip was placed on a hot plate and incubated at 37℃. To provide nutrients, liquid CAMHB medium was supplied from the side-branched channels. The growth of the bacteria was monitored by using a microscope. Bacterial growth was not inhibited and could be clearly monitored according to the incubation time for the MAC system (Fig. 3.4). There were two types of bacterial

growth in the MAC system. The dividing type (one red circle in Fig. 3.4C) is well known and normal, but the aggregative type (two blue circles in Fig. 3.4C) has not been reported thus far in *in vitro* culture systems. We speculate that the abnormal cell growth type (aggregative type) could be classified as a type of biofilm formation [19]. The aggregative type of cell growth is being investigated further.

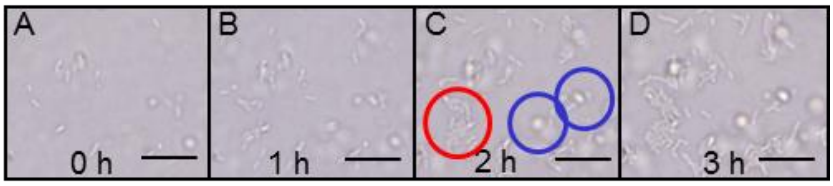

Figure 3.4 Fixation and tracking of the growth of bacteria in the microfluidic agarose channel (MAC) system. Using time lapse images obtained with by microscopy, the growth of the bacteria was monitored. The bacteria were fixed firmly and grew well in the solidified and thin agarose matrix. Two types of cell growth occurred in the MAC system: dividing type (one red circle) and aggregative type (two blue circles). The scale bars represent 20 μm [8].

3.2.3 Image Processing

Bacterial cell images were taken with a CCD camera; the images were then processed to determine the MIC values of the antibiotics. The image data were transformed into digital data using our own image processing program, which is coded in Matlab (Fig. 3.5). For the calculations, RGB images (Fig. 3.5A) were transformed into grey formatted images (Fig. 3.5B). The background of each image was differentiated from the bacteria and then eliminated (Fig. 3.5C). Then, the contrast was enhanced by adjusting function. Following this, the processed images were changed into binary format images (Fig. 3.5E) [20]. The processing program calculated the areas that were occupied by each bacterium. A longer incubation time allowed each bacterium to grow and occupy more area. When the cells grew in the agarose matrix, they did so by following two types of cell growth: dividing type and aggregative type (Fig. 3.4). The imaging processing program worked well for both the dividing and aggregative types of growth, because it measured the sizes of the regions that the bacteria occupied. After image processing, the area occupied by bacterial growth was calculated. The proportional growth rate of the bacterium was subsequently calculated by using Eqn. 2.2 and then plotted against the incubation time.

$$\text{Proportional Growth Rate of Bacteria} = \frac{A_t - A_0}{A_0} \tag{2.2}$$

A_t and A_0 are the areas of the image that are occupied by a bacterium at

time t and the initial state (0 h), respectively. By observing the growth rate on the graph, the susceptibility of the bacteria to an antibiotic can be determined.

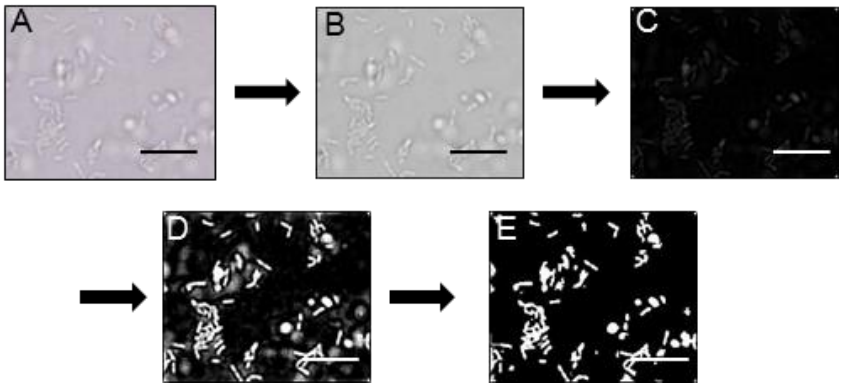

Figure 3.5 Image processing. RGB images (A) were transformed into grey format images (B). The background was eliminated (C) and optimized (D). The processed images were changed into binary format images to enhance the image contrast (E). The scale bars represent 20 μm [8].

3.2.4 AST with the PDMS MAC system

To validate the MAC system for AST, three standard CLSI bacteria (*E. coli* ATCC 25922, *S. aureus* ATCC 29213, and *P. aeruginosa* ATCC 27853) were tested to determine the MICs of amikacin, norfloxacin, tetracycline, and gentamycin. The CLSI is recognized worldwide and provides information and AST data on clinical bacteria using a standard AST method for quality control. We followed the CLSI method for bacterial cell preparation, culturing, and the microdilution AST.

Among the three CLSI standard bacteria, *P. aeruginosa* ATCC 27853 is Gram-negative, aerobic, and among the most common human pathogens because it causes a variety of nosocomial infections, including pneumonia, urinary tract infections, surgical wound infections, and bloodstream infections [21]. *E. coli* ATCC 25922 is also a Gram-negative bacterium, and most *E. coli* strains do not cause diseases. However, some strains can cause serious food poisoning in humans [22]. *S. aureus* ATCC 29213 is a Gram-positive, facultative anaerobic bacterium. It is involved in a broad range infections and causes various life-threatening diseases such as sepsis, pneumonia, meningitis, and endocarditis [23, 24]. MRSA and VRSA are leading antibiotic-resistant strains present in hospitals [25, 26].

The MIC values of gentamycin against *S. aureus* ATCC 29213 and *P. aeruginosa* ATCC 27853 that were determined by using the MAC system are shown in Fig. 3.6A and 3.6B, respectively. The images were taken at the same position

every hour using a time lapse method. In the CLSI report, the MIC values are in the range 0.12–1 μg/ml (gentamycin against *S. aureus*) and 0.5–2 μg/ml (gentamycin against *P. aeruginosa*). The tested concentrations of gentamycin were determined to be in the ranges 0–2 μg/ml for *S. aureus* and 0–4 μg/ml for *P. aeruginosa*. Liquid CAMHB medium containing different concentrations of gentamycin were supplied from the side-branched channel into the main channel through diffusion. After 3 hours incubation, there were noticeable differences among the images. In the case of *S. aureus* ATCC 29213, the images for below 1 μg/ml showed that the bacteria grew and occupied more space. However, for the images over 1 μg/ml, the bacteria did not grow and remained in the same state. After image processing, we plotted the proportional growth rate of the bacteria that we could derive on the graph as a function of the incubation time (Fig. 3.6A). The sizes of the areas occupied by the bacteria did not change for 1 and 2 μg/ml (*S. aureus* ATCC 29213) and 2 and 4 μg/ml (*P. aeruginosa* ATCC 27853); however, below 1 μg/ml (*S. aureus* ATCC 29213) and 2 μg/ml (*P. aeruginosa* ATCC 27853), the areas increased linearly. From the data, we determined the MIC value of gentamycin against *S. aureus* ATCC 29213 to be 1 μg/ml and that of gentamycin against *P. aeruginosa* ATCC 27853 to be 2 μg/ml. The MIC values were in the MIC ranges of the CLSI data.

Furthermore, the MIC values of amikacin, norfloxacin, tetracycline, and gentamycin against the three CLSI strains were also determined within a few hours

(3 or 4 h). The MIC values were verified using the microdilution method and compared with the MIC data of the CLSI. All MIC data for the MAC system were in the MIC ranges of the CLSI results (Table 3.1). From these results, the MAC system reduced the AST time for MIC determination and generated accurate MIC data in a microfluidic environment. In the case of norfloxacin against *S. aureus* ATCC 29213, it took seven hours to determine the MIC. In the norfloxacin environment, *S. aureus* ATCC 29213 tended to grow slowly over the MIC, which showed that it took relatively more time for AST than that required for the AST system. The time for determining the MIC could be reduced by using a high resolution image system and optimized image processing via the MAC system.

Tuson et al.[27] demonstrated that bacterial cell growth was partially inhibited in 2% agarose. In our work, bacterial cells were incubated in 1.5% agarose. There was not significant growth inhibition that could influence on the MIC determination in the MAC system.

We analyzed the growth of bacteria that are tolerant to low concentrations of oxygen. The PDMS channel is gas permeable[28] and *Bacillus subtilis* ATCC 6633 (an obligate aerobic bacterium) was tested and grew well in the MAC system, resulting in the same MIC value of kanamycin (6.25 μg/ml) as that from the micro-dilution test. In addition, we presume that sufficient oxygen can be solved in the supplied fresh liquid medium. Therefore, The MAC system also can be used with

obligate aerobic bacteria.

In this research, only six kinds of concentration could be tested on single chip in the MAC system. The system required a syringe pump system with laborious works such as connecting tube and controlling flow rate. However, in clinical area, more multiplexed, high throughput and user-friendly systems are needed. In the MAC system, the number of the channel can be expanded and additionally the automated imaging system can be introduced. The improvements of the channel design and antibiotic delivery without external instruments and automation of the imaging system will enable the MAC system to be practically used in the hospital.

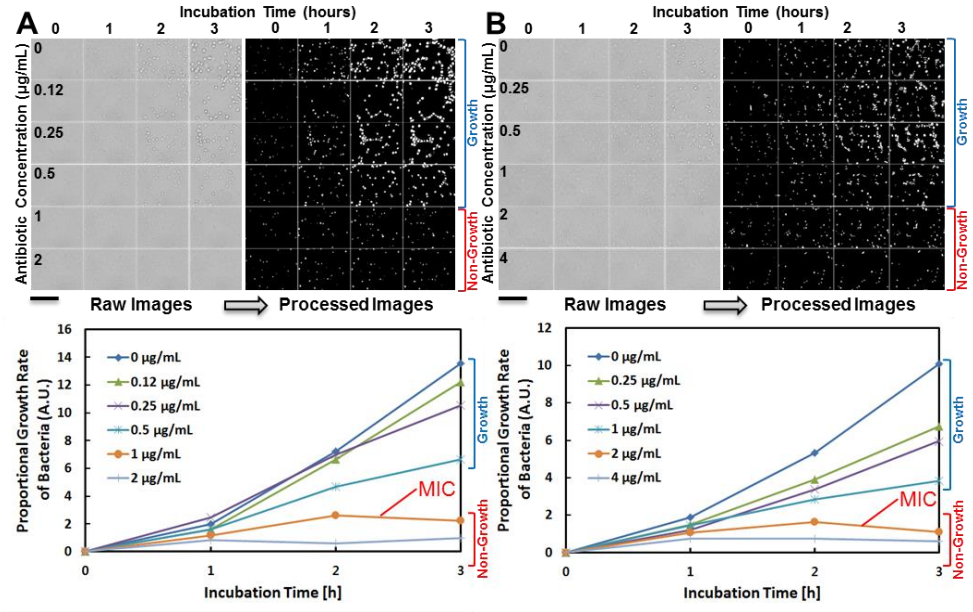

Figure 3.6 Minimal inhibitory concentration (MIC) determination through image processing. (A) The MIC determination of gentamycin against *S. aureus* ATCC 29213. After image processing, the bacteria that occupied the area were measured and plotted on the graph for different concentrations of gentamycin according to the incubation time. The 1 μg/ml and 2 μg/ml concentrations did not permit bacterial growth, whereas the other concentrations increased bacterial growth according to the incubation time. From this data, the MIC of gentamycin against *S. aureus* ATCC 29213 was determined to be 1 μg/ml (B) The MIC determination of gentamycin against *P. aeruginosa* ATCC 27853. In the same procedure as that stated above, the MIC of gentamycin against *P. aeruginosa* ATCC 27853 was determined to be 2 μg/ml. The scale bars represent 50 μm [8].

Table 3.1 A comparison of the minimum inhibitory concentrations between the Clinical and Laboratory Standard Institute (CLSI) method and the microfluidic agarose channel system for 3 CLSI standard strains (units: μg/ml). [a]Time: Time required to determine the MIC (h) [8].

	Escherichia coli ATCC 25922		*Staphylococcus aureus* ATCC 29213	
Antibiotics	CLSI	RAST (Time[a])	CLSI	RAST (Time)
Amikacin	0.5–4	4 (3 h)	1–4	4 (3 h)
Norfloxacin	0.03–0.12	0.03 (4 h)	0.5–2	0.5 (7 h)
Tetracycline	0.5–2	1 (3 h)	0.12–1	0.5 (3 h)
Gentamycin	0.25–1	1 (4 h)	0.12–1	1 (3 h)

	Pseudomonas aeruginosa ATCC 27853	
Antibiotics	CLSI	RAST (Time[a])
Amikacin	1–4	4 (3 h)
Norfloxacin	1–4	0.03 (4 h)
Tetracycline	8–32	1 (3 h)
Gentamycin	0.5–2	1 (4 h)

3.3 Summary

In summary, I designed a microfluidic agarose channel system called MAC, which can reduce the time taken for AST. For this system, microchannels are integrated with solidified agarose. Bacteria are fixed in a thin agarose matrix, and different concentrations of antibiotics are supplied to the bacteria by diffusion. The growth of single bacterial cells is tracked by microscopy according to the incubation time, and the images are processed through our own image processing program to determine MIC values. The entire AST process takes 3–4 h, and it produces data that is comparable in accuracy to the conventional AST results of the CLSI.

In the clinical setting, the MAC system can produce rapid and accurate AST data for determining proper medication doses. It can be used to avoid the overuse or misuse of antibiotics and save many patients from death.

Chapter 4

Single-Cell Morphological Analysis

In the chapter 3, I reported that tracking single cell growth in microfluidic channel determined drug susceptibility by calculating the bacteria-occupying area in the images [8]. These tests determine antimicrobial susceptibility based on the simple observation of whether the bacteria are growing. However, the antimicrobial responses of bacteria are very heterogeneous and specific to different antibiotic conditions [29, 30]. We therefore hypothesized that a more accurate characterization of the "response" would include morphological changes.

In this chapter, I demonstrated the clinical application of a rapid AST with imaging-based single-cell morphological analysis (SCMA). SCMA can determine antimicrobial susceptibility by analyzing the morphological changes of single bacterial cells under various conditions. To adapt the SCMA to a high-throughput format, we developed a microfluidic chip that molds bacteria-mixed agarose to a

thin, flat microscale slab. Thousands of morphological change patterns were acquired performing time-lapse bright-field imaging of single-cells using the microfluidic chip. From the results, we categorized the response of bacteria into several different morphological patterns. These patterns from our SCMA system were then correlated with the broth microdilution (BMD) test, which serves as the clinical gold standard. To eliminate human error in morphological analysis, we developed an automated image-processing and classifying algorithm that determines bacterial resistance to antibiotics.

4.1 AST process in the Plastic MAC system

4.1.1 Microfluidic agarose channel (MAC) integration with a 96-well format

Bacterial cells that are “resistant” to an antibiotic can divide in the presence of the drug. In contrast, “susceptible” bacterial cells are not able to divide because their growth is inhibited by bacteriostatic or bactericidal effects. Therefore, observing bacterial cell division is a fundamental method for determining bacterial resistance or susceptibility to antimicrobial agents. Turbidity, as determined by optical density (OD), is typically measured either by bare eyes or spectrophotometer to determine the bacterial cell division under antimicrobial conditions. Conventional clinical AST platforms typically use this OD method, where changes in OD reflect bacterial growth and, hence, drug resistance. However, owing to the high limit of detection of OD-based methods ($\geq 10^7$ CFU/ml), ASTs take 16~20 hours for sufficient bacterial growth (Fig. 4.1A).

To overcome this limitation, methods were developed to track the growth of single bacterial cells. However, it is difficult to apply such methods to ASTs because many types of motile bacteria cannot easily be observed and tracked. To observe and track single bacterial cells in a clinic-ready AST systems, we needed to: 1) immobilize bacteria, 2) provide a stable supply of nutrients and antimicrobial agents, 3) make imaging convenient and easy, and 4) make the AST high-throughput. We designed a microfluidic chip that immobilizes bacterial cells in agarose, to facilitate

image-based monitoring of single bacterial cell growth [8], that integrated it with a 96-well format for high-throughput testing (Fig. 4.1B; Fig. 4.2).

In the MAC chip, nutrients and antimicrobial agents were supplied to the bacterial cells in the channel without any external equipment via diffusion (Fig. 4.1B) [31-33]. To perform a rapid AST in 3 hours, the diffusion of antimicrobials into the imaging region needs to be complete in 20 to 30 minutes, considering the division time of bacterial cells. The region of interest for imaging in the MAC chip was a square region (200 μm x 200 μm) of the interface between the agarose matrix and the antibiotic well. Approximate diffusion times of the antibiotic penicillin, and amino acids and proteins [lysozyme, formyl-norleucyl-leucyl-phenylalanine (FNLLP), bovine serum albumin (BSA)] into imaging area were <5 minutes, indicating that the diffusion is sufficiently fast for AST, considering bacterial dividing times (~20 min) (Table 4.1).

The bacterial cell samples were mixed with 1.5% liquid agarose at 37℃ and then loaded into the well inlets to form MACs surrounding the liquid medium sample wells (Fig. 4.1C). As the agarose solidified in the channels at room temperature, the bacterial cells became immobilized. The liquid medium samples [Mueller Hinton Broth (MHB) containing various antimicrobial agents at different concentrations] were then applied to the different wells. The agents and nutrients diffused from the antibiotic well towards the bacterial cells in the channels

(characterized for Rhodamine B in Fig. 4.3). About 30 combinations of antimicrobial agents (Table 4.2) and test strains were loaded at the same time and subjected to SCMA by time-lapse imaging at 0, 2, and 4 hours for Gram-positive strains *S. aureus* and *Enterococcus* spp. and at 0, 1.5, and 3 hours for Gram-negative strains *E. coli, Pseudomonas aeruginosa* and *Klebsiella pneumoniae*

The bacterial cells growing on the bottoms of the channels in the boundary areas between the liquid medium samples and the MACs were imaged by time-lapse method to monitor the change in bacterial morphology (Fig. 4.1B and 4.1C). We took bacterial growth images of six different areas in the boundary region (1 mm x 1 mm) between the microfluidic channel and the well under/at MIC conditions. The pattern of bacterial growth did not exhibit any differences in these four areas in the vicinity of the well with the antibiotics; however, bacteria in regions farther from the antibiotics were unresponsive (Fig. 4.4). We therefore chose the region closest to the antibiotic well to take images and obtain reliable AST results. We took one image (area 200 μm x 200 μm) per well for SCMA, with each field of view containing tens of bacterial cells.

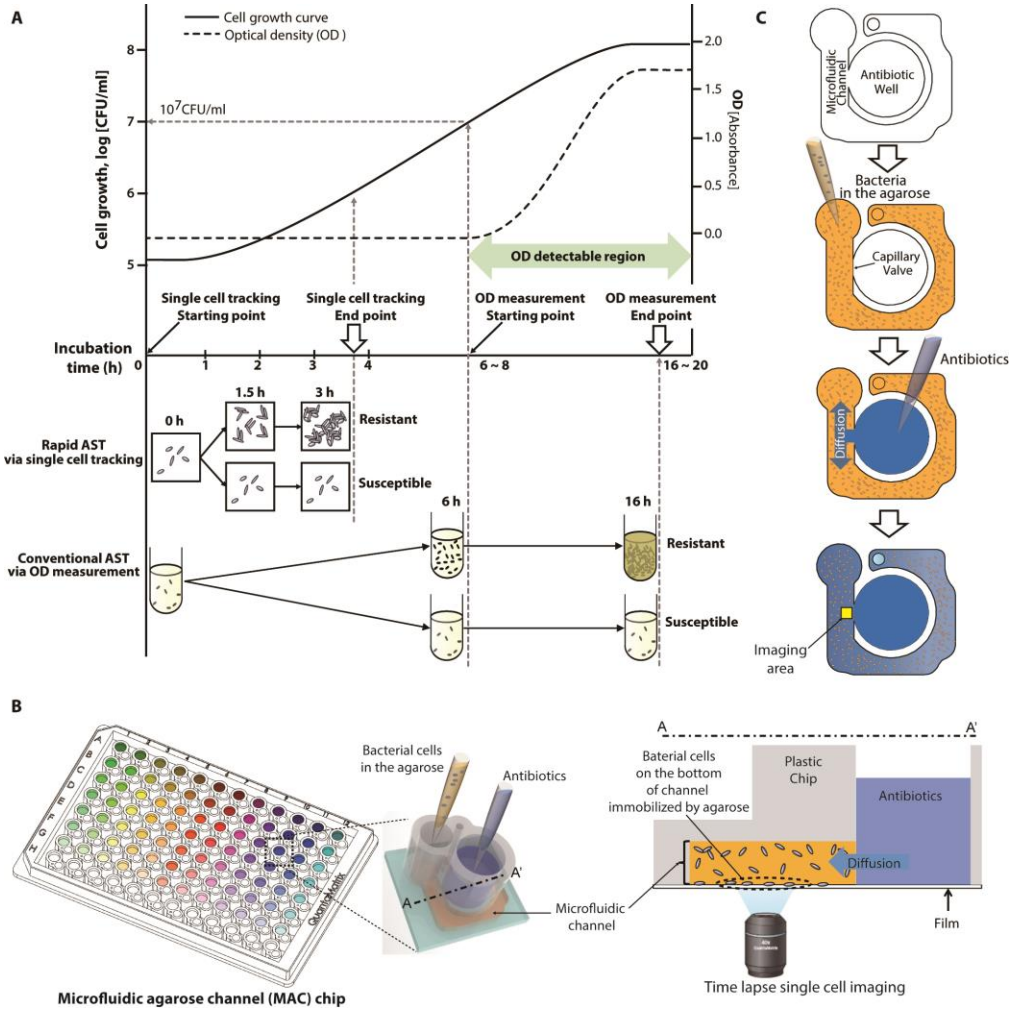

Figure 4.1 The rapid AST platform uses single bacterial-cell morphology tracking in microfluidic agarose channels. (A) Comparison of an AST based on single-cell morphological analysis (SCMA) with the conventional method using optical density (OD) measurements. In principle, the SCMA method reduces the AST time compared with conventional OD-based AST. In conventional AST by OD measurement, the OD value does not change until the bacterial concentration

reaches 10^7/ml, so OD measurement cannot be performed for 6~8 hours [34]. However, in single-cell tracking using a microscope, changes in bacterial cells can be detected as soon as cells divide, so antibiotic susceptibility can be determined in 3~4 hours. (B) Schematic of the microfluidic agarose channel (MAC) chip integrated with a 96-well platform for high-throughput analysis. The MAC chip is composed of microfluidic channels containing bacteria in agarose, and a well to supply antibiotics and nutrients. The imaging region was the interface between the liquid medium and the microfluidic channel. The immobilized bacterial cells on bottoms of channels were monitored for SCMA by time-lapse bright field microscopy. Detailed well dimensions and interfacing with 96-well plates are in Fig. 3.2. (C) Experimental procedure for the MAC chip. Bacterial cells were mixed with agarose and loaded into a microfluidic channel, where the cells were immobilized by gel solidification. Liquid nutrients, some spiked with antimicrobials, were then loaded into the wells. These liquid samples diffuse into the agarose through openings between the channels and the wells. Time-lapse imaging was performed in the imaging region (yellow box). Scale bar, 20 μm [35].

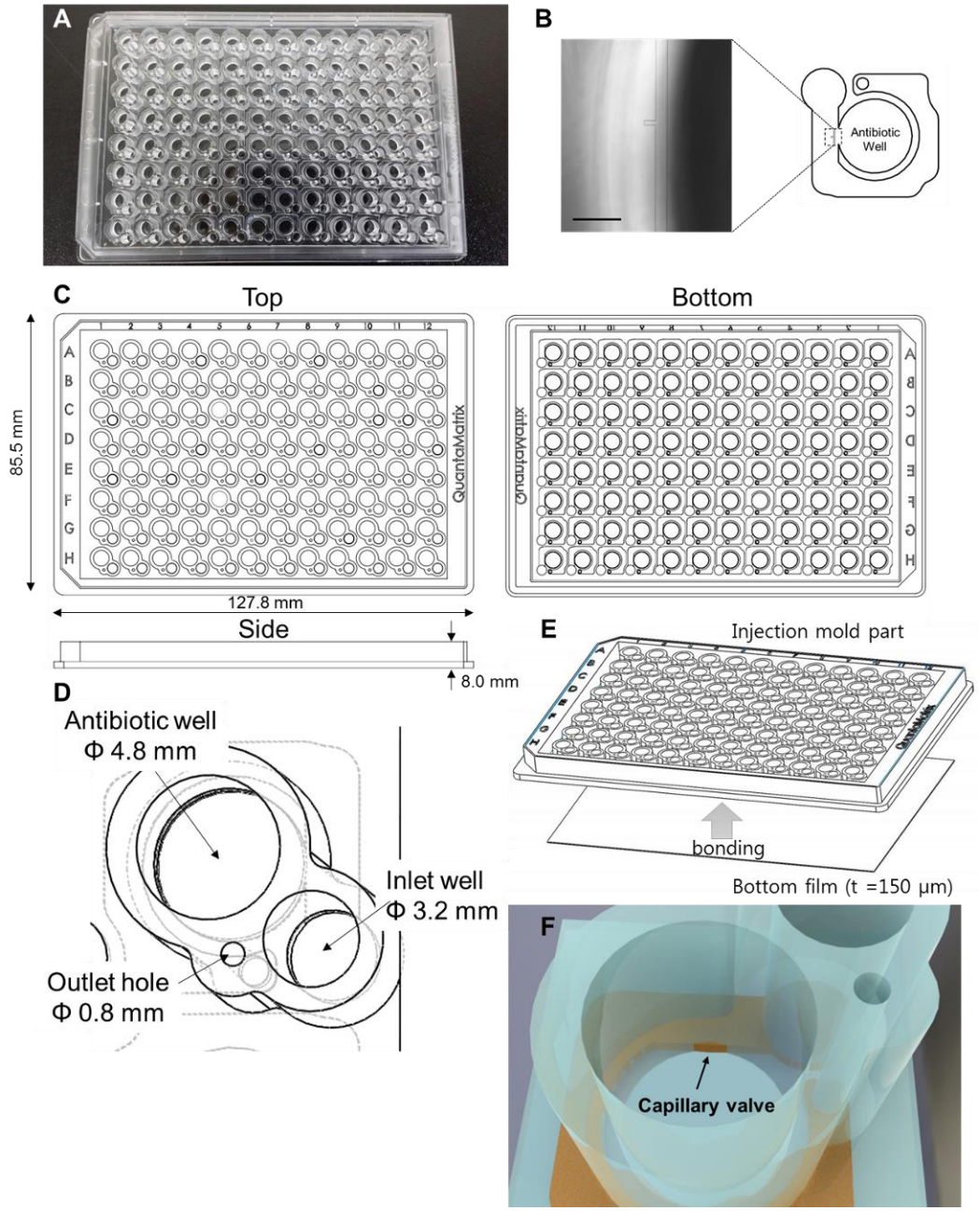

Figure 4.2 MAC chip. (A) The MAC chip is in a 96-well format and was made by an

injection-molding process. (B) For automatic imaging, a focus mark (12 μm × 200 μm) was imprinted on the bottom of the film. Scale bar, 50 μm. (C) The schematic view of the MAC chip. The dimensions of the chip are 127.8 mm × 85.5 mm (same as conventional 96-well plate) and 8.0 mm of height. (D) The dimensions of the wells in the MAC chip. (E) The process of bonding of injection mold part [polycarbonate] and bottom film [poly(methyl methacrylate), thickness : 150 μm]. (F) Detailed view of capillary valve [35].

4.1.2 Diffusion characteristics in agarose within the MAC chip

Generally, when a molecular species diffuses into a substance, a concentration gradient of that molecular species is generated in the substance. However, at the interface between the molecular source and the substance, the molecular concentration can be assumed to be the same as at the source. To verify this assumption, we approximated the diffusion time. The diffusion coefficient of penicillin (MW = 313) in 2.0% agarose at 37℃ is approximately 4.4×10^{-6} cm^2/s (*21*). The diffusion coefficient of amino acid (formyl-norleucyl-leucyl-phenylalanine (FNLLP), MW = 421 Da) in 0.5% agarose at 37℃ is approximately 1.0×10^{-5} cm^2/s

(*22*). Additionally, diffusion coefficients are 7.12×10^{-7} cm^2/s for bovine serum albumin (BSA) and 1.48×10^{-6} cm^2/s for lysozyme in 1.0% agarose at 37℃ (*23*). From these diffusion coefficients, the diffusion time of the molecules can be approximated using the equation $t = x^2/2D$, where t, x, and D are time, distance of diffusion, and diffusion coefficient, respectively. This provided the diffusion time into the imaging region (200 μm) of the interface in the MAC chip.

Table 4.1 Diffusion times into the imaging region. The imaging region was 200 μm x 200 μm [35].

Substance	Diffusion coefficient (cm^2/s) (% of agarose)	Diffusion time into the imaging region (min)
Penicillin	$4.4x10^{-6}$ (2)	0.8
FNLLP	$1.0x10^{-5}$ (0.5)	0.3
BSA	7.12×10^{-7} (1.0)	4.7
Lysozyme	1.48×10^{-6} (1.0)	2.3

Table 4.2 Molecular weights of antimicrobial agents tested in the clinical AST. The antimicrobial solution was diffused into the solidified agarose containing bacteria. The molecular weight of antimicrobials is an important parameter for calculation of diffusion characteristics [35].

Antimicrobial	**Molecular weight (Da)**
Amikacin	585.6
Amoxicillin/clavulanic acid	365.4/199.2
Ampicillin	349.4
Ampicillin/sulbactam	349.4/233.2
Aztreonam	435.4
Benzylpenicillin	334.4
Cefazolin	454.5
Cefepime	480.6
Cefotaxime	455.5
Cefotetan	575.6
Cefoxitin	427.5
Cefpodoxime	427.5
Ceftazidime	546.6
Ceftriaxone	554.6
Cefuroxime	424.4
Ciprofloxacin	331.3
Doripenem	420.5
Daptomycin	1619.7
Ertapenem	475.5
Erythromycin	733.9
Gentamicin	477.6
Imipenem	299.3

Levofloxacin	361.4
Linezolid	337.4
Meropenem	383.5
Minocycline	457.5
Moxifloxacin	401.4
Nitrofurantoin	238.2
Norfloxacin	319.3
Piperacillin	517.6
Sulbactam	233.2
Quinupristin/dalfopristin	1022.2/690.9
Rifampicin	822.9
Streptomycin	581.6
Telithromycin	812.0
Tetracycline	444.4
Ticarcillin	384.4
Ticarcillin/clavulanic acid	384.4/199.2
Tigecycline	585.7
Tobramycin	467.5
Trimethoprim	290.32
Trimethoprim/sulfamethoxazole	290.3/253.3
Vancomycin	1449.3

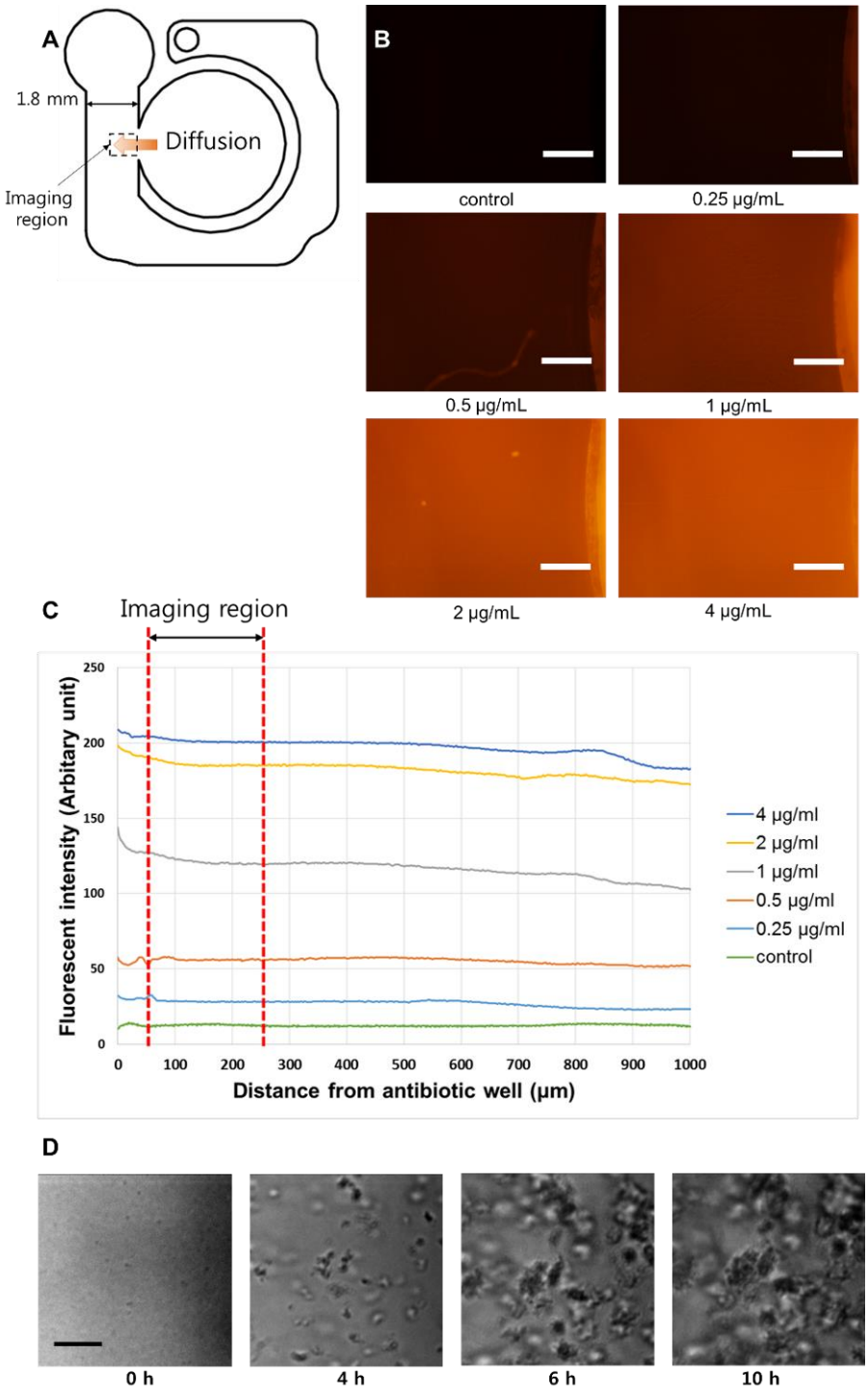
A
1.8 mm
Diffusion
Imaging region
B
control
0.25 μg/mL
0.5 μg/mL
1 μg/mL
2 μg/mL
4 μg/mL
C
Imaging region
Fluorescent intensity (Arbitary unit)
Distance from antibiotic well (μm)
4 μg/ml
2 μg/ml
1 μg/ml
0.5 μg/ml
0.25 μg/ml
control
D
0 h
4 h
6 h
10 h

Figure 4.3 Diffusion characteristics of Rhodamine B in the imaging area of the MAC chip. After the loading of pure agarose, a fluorescent dye (rhodamine B, MW: 479.0 Da) was injected at various concentrations into the antimicrobial wells. The images were taken 30 minutes after the loading of the dye. (A) Schematic of the imaging region and the direction of flow. (B) Fluorescence images of the imaging region. The exposure time was set to 300 ms. Scale bars, 250 μm. (C) Fluorescence intensity as a function of distance from the antibiotic well containing Rhodamine B. (D) Long term time-lapse images of *E. faecalis.* Scale bar, 25 μm [35].

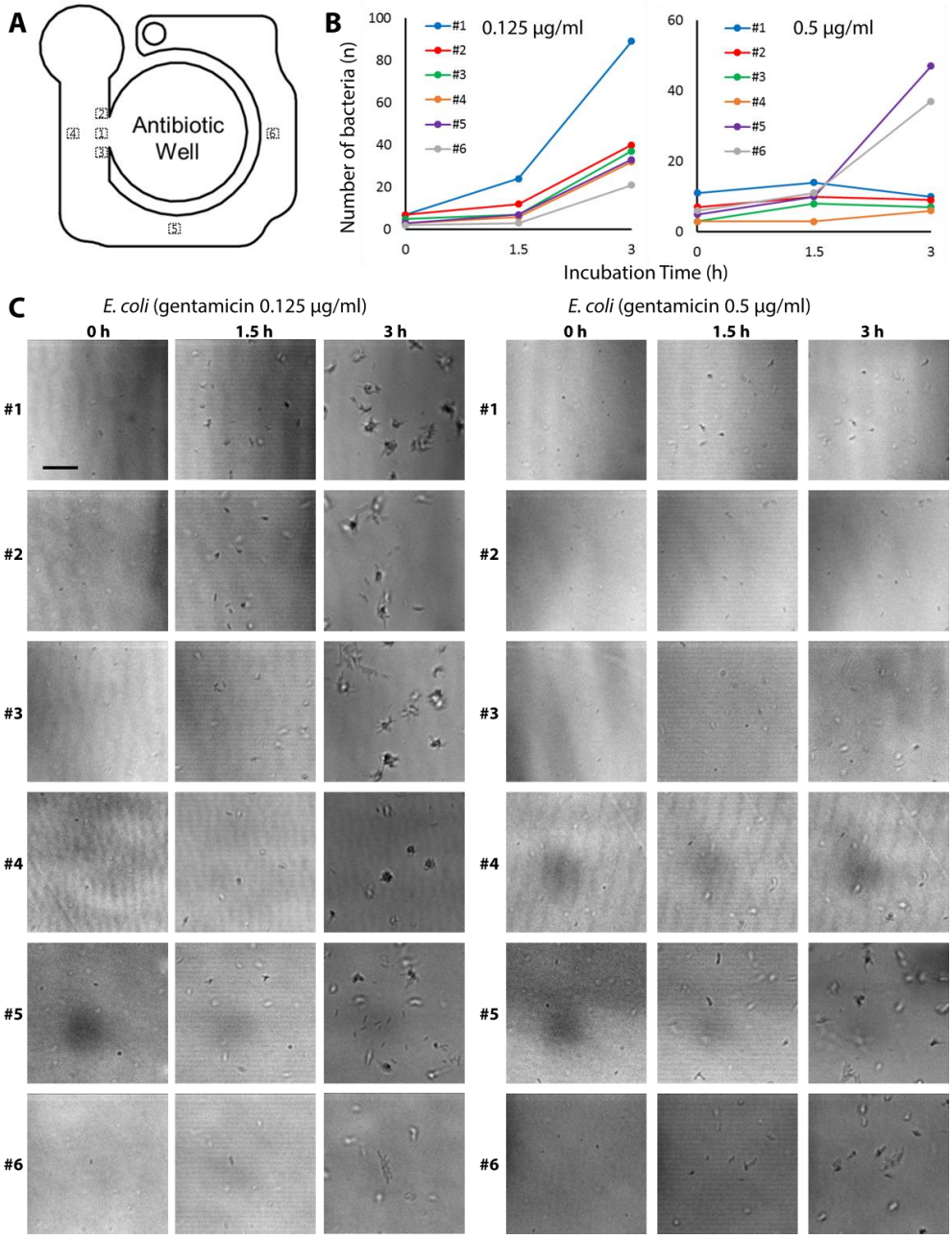

Figure 4.4 Time-lapse images of bacteria at the different locations in the MAC chip. (A) The six different imaging regions. (B) The number of bacteria according to the

each region. (C) Time-lapse images of *E. coli* ATCC with gentamicin at the different locations. In regions 1–4, near the antibiotic well, the responses of the bacteria were identical. In regions 5 and 6, the bacteria divided regardless of antibiotic concentration. Scale bar, 25 μm [35].

4.2 Single-cell morphological analysis (SCMA) for rapid and accurate AST

4.2.1 Development of SCMA

We tested four clinically relevant [36, 37] and standard CLSI strains—*E. coli* ATCC 25922, *S. aureus* ATCC 29213, *P. aeruginosa* ATCC 27853, and *E. faecalis* ATCC 29212—in our MAC chip with imaging. The antimicrobial agents to be tested on each strain were selected according to the lists of commercial AST kits from Vitek 2 systems (bioMérieux Inc.) and MicroScan WalkAway (Siemens Healthcare Diagnostics). Time-lapse images of bacterial cell growth were obtained to determine the MIC for the four strains. Bacterial imaging for AST was performed three hours after drug administration to Gram-negative strains and four hours after for Gram-positive strains because the growth rates differ.

From the time-lapse images, the MICs were determined using a previously developed image processing method (bacterial area measuring (BAM) method) [8] which determined the antimicrobial susceptibility only by measuring the cell mass in the images as other single cell imaging methods for AST [38-40]. If the bacterial area in the images increased, the case was determined as “resistant” and if the bacterial area was static, the cases was determined as “susceptible”.

As typical case, in the case of gentamicin against *P. aeruginosa* ATCC 27853, bacterial area in the images increased with incubation time under 1.0 μg/ml. From 1.0 μg/ml, the bacterial area were not changed. Therefore, 1.0 μg/ml was

determined as the MIC value by the BAM method. The value was agreed with the MIC value from the BMD and the MIC value was within the CLSI QC range (0.5 ~ 2 μg/ml, [41]) (Fig. 4.5A).

In the cases of ceftazidime against the same strain, however, bacterial area in the images increased in all concentrations showing filamentary formations and the MIC could be higher than 8.0 μg/ml by the BAM method. The MIC value was not matched to the BMD result (2 ~ 4 μg/ml) and was not within the CLSI QC range (1 ~ 4 μg/ml) (Fig. 4.5B). The mismatch of the MIC value was also occurred in the case of imipenem against the same strain showing swelling formations (Fig. 4.5C). We found that in the case of the β-lactam antimicrobial agent against Gram-negative strains such as *E. coli* ATCC 25922 and *P. aeruginosa* ATCC 27853, the MIC was discordant with the BMD test because filamentary or swelling formation caused increase of the bacterial occupying area at/above the MIC value. It suggested that the BAM method was not able to determine the MIC value and susceptibility in accordance to BMD test. It is desired that new AST method that can cope with very heterogeneous bacterial response to different antibiotics [29, 30].

We proposed and demonstrated here a single-cell morphological analysis (SCMA) as new image based AST method that meets the accuracy requirements of AST by observing morphological changes of bacterial single cell under various antimicrobial conditions. Instead of applying same judging criteria of change in cell

mass to all combination of bacterial strains and antibiotics as in case of BAM, we classified antibiotic responses of bacteria to multiple cases and applied different judging criteria considering both changes in cell mass and morphology. We investigated the correlation between SCMA and the BMD test results and verified that the MIC values from SCMA were within the CLSI quality control (QC) range for various antimicrobials. To analyze single-cell morphology under different concentrations of antibiotics, bacterial cell numbers and sizes were measured. For instance, In the case of ceftazidime against the same strain, the cell numbers increased while the sizes were not changed under 2 μg/ml. From 2 μg/ml, there was no change in the cell numbers, but the cell sizes increased showing the filamentary formation. Considering the BMD result (2 ~ 4 μg/ml) and the CLSI QC range (1 ~ 4 μg/ml), 2 μg/ml was determined to be the MIC value (Fig. 4.5B).

In the case of imipenem against the same strain, the cell numbers increased, while the cell sizes did not change under 1 μg/ml. From 1 μg/ml, the cell numbers were not changed, but the cell sizes increased showing swelling formation. 1 μg/ml was determined as the MIC value. The MIC value was a little different with that of the BMD result (2 ~ 4 μg/ml), but the value was in the CLSI QC range (1 ~ 4 μg/ml) (Fig. 4.5C). To determine the MIC values of the other antimicrobial agents, the morphological analysis was applied by considering the BMD results and the CLSI QC range (Tables 4.3, 4.4 and 4.7, Fig. 4.6). The cases of Gram-positive strains (*S.*

aureus ATCC 29213 and *E. faecalis* ATCC 29212) mainly consisted of dividing or non-dividing cases without size change. However, the growth rates of bacteria in the various antimicrobial agents were different. When the growth rate of the strains differed, the MIC values were determined by comparing the relative growth rate in different concentrations of antimicrobial agents (Table 4.5, 4.6 and 4.7, Figs. 4.7 and 4.8).

The discordant MIC values from the BAM method were re-evaluated and all of the MIC values were found to be within the quality control ranges from the CLSI, except *E. faecalis* ATCC 29212 with erythromycin. In this case, the MIC value was lower than the CLSI MIC quality control range. This may have resulted because *E. faecalis* ATCC 29212 had relatively slow growth under erythromycin (Table 4.6) making it difficult to observe the change in 4 hours. However, in clinical test, susceptibility was well determined using clinical strain *E. faecalis* with erythromycin.

After testing most of clinically used antibiotics to many clinical strains, the bacterial cell morphologies were categorized into six types for SCMA: dividing, no change, filamentary formation, swelling, co-existence of filamentary formation and dividing, or swelling formation and dividing (Fig. 4.9). The typical dividing pattern in the antibiotic-free and the antibiotic-resistant conditions involved single bacterium dividing into two cells, which increased both the number of bacterial cells

and the OD value of the BMD test (Fig. 4.5A, Fig. 4.9A). The typical pattern in the susceptible condition involved no change in the bacterial cells (Fig. 4.9B). Filamentary formation occurred for Gram-negative strains in response to most β-lactam antimicrobial agents, with the exception of the penem class drugs (Fig. 4.9C). These bacterial cells typically showed filamentary formation but no division. Swelling patterns were observed for Gram-negative strains in response to the penem class drugs (imipenem and meropenem) (Fig. 4.9D). These bacterial cells were swollen but did not divide. In the illustrated cases of filamentary and swelling formations (Fig. 4.9C to 4.9D), we chose to determine the bacteria to be "susceptible" to the antibiotics because there was no OD change. This is because no OD change in the conventional BMD test would also give out "susceptible". For cases in which we observed the co-existence of filamentary formation and dividing or swelling formation and dividing, we determined that the bacteria were resistant (Fig. 4.9E and 4.9F).

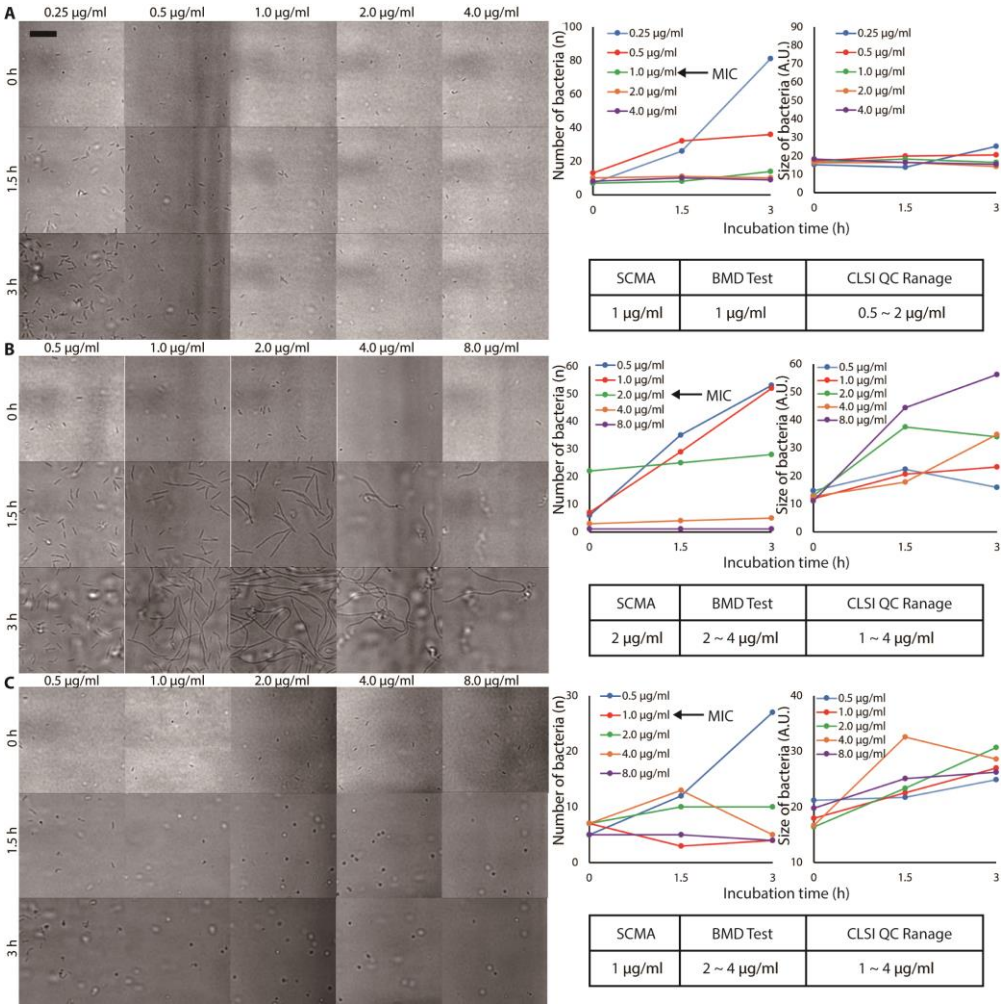

Figure 4.5 MIC determination analyzing bacterial number and size with *P. aeruginosa* ATCC 27853. (A) In the case of Gentamicin. At concentrations lower than 1.0 μg/ml, bacterial cells divided. However, at concentrations equal to or higher than 1.0 μg/ml, the bacterial cells stopped dividing. 1.0 μg/ml was determined as the MIC value and the MIC value was within the CLSI QC range (0.5-2 μg/ml). (B) In the case of ceftazidime. At lower concentration than 2 μg/ml, the bacterial cells

divided. At concentrations equal to or higher than 2 μg/ml, ceftazidime induced filament formation (cell elongation), but the bacterial cells did not divide. 1.0 μg/ml was determined as the MIC value within the CLSI QC range (1-4 μg/ml). (C) In the case of imipenem. At concentration lower than 1.0 μg/ml, the bacterial cells were divided. At concentrations equal to or higher than 1.0 μg/ml, imipenem induced cell swelling, resulting in cells bursting, and bacterial cells did not divide. 1.0 μg/ml was determined as the MIC value within the CLSI QC range (1-4 μg/ml). Additional morphological data are provided in table S4. Scale bar, 25 μm [35].

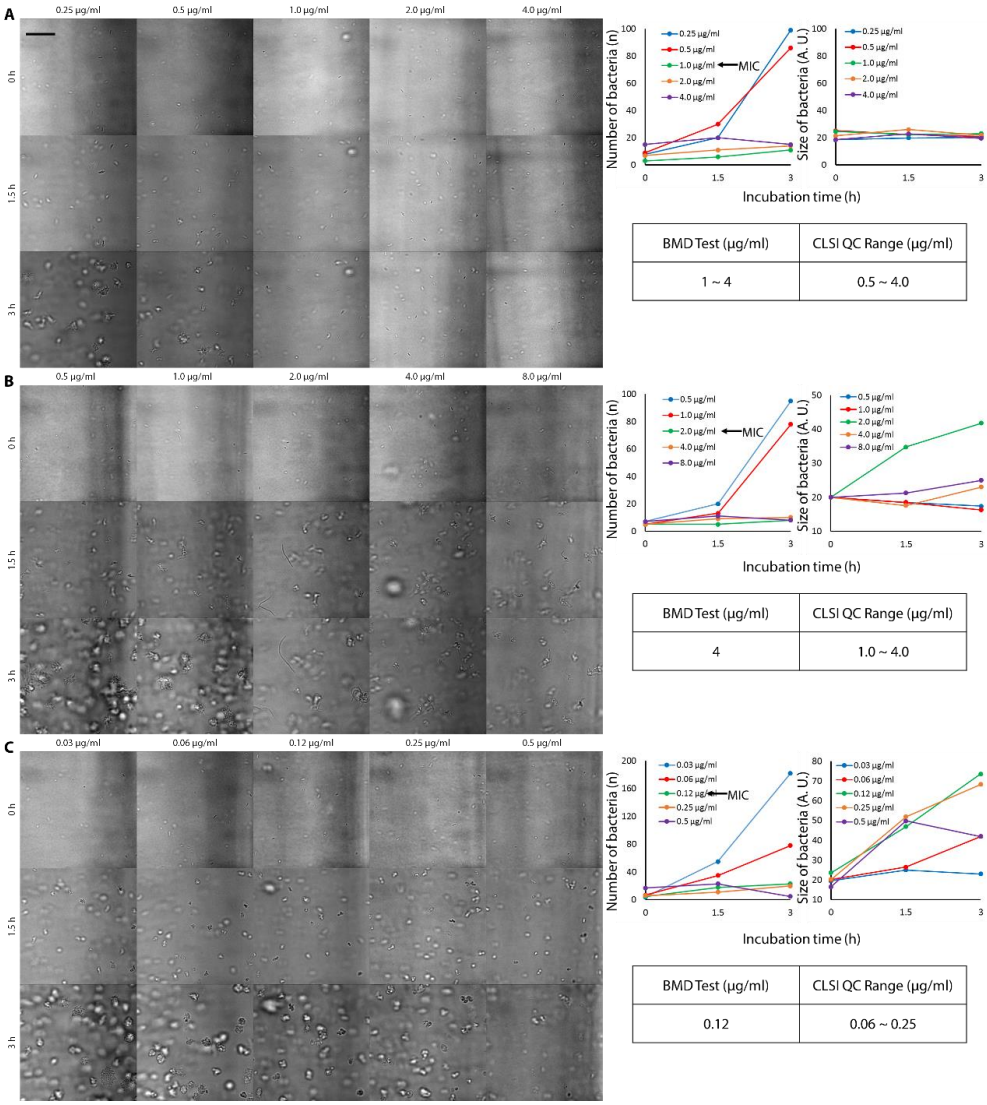

Figure 4.6 MIC determination analyzing bacterial number and size with *E. coli* ATCC 25922. (A) In the case of amikacin. At concentrations lower than 1.0 μg/ml, bacterial cells divided. However, at concentration equal to or higher than 1.0 μg/ml, the bacterial cells stopped growing. 1.0 μg/ml was determined as the MIC value and the MIC value was within the CLSI QC range (0.5-4.0 μg/ml). (B) In the case of

piperacillin. At lower concentrations than 2.0 μg/ml, the bacterial cells were divided into two cells. At concentrations equal to or higher than 2.0 μg/ml, piperacillin induced filament formation (cell elongation), but the bacterial cells did not divide. 2.0 μg/ml was determined as the MIC value and the MIC value was within the CLSI QC range (1.5-4.0 μg/ml). (C) In the case of imipenem. At concentration lower than 0.12 μg/ml, the bacterial cells divided. At concentrations equal to or higher than 0.12 μg/ml, imipenem induced cell swelling, resulting in cells bursting, and bacterial cells did not divide. 0.12 μg/ml was determined as the MIC value and the MIC value was within the CLSI QC range (0.06-0.25 μg/ml). Additional morphological data are in table S3. Scale bar, 50 μm [35].

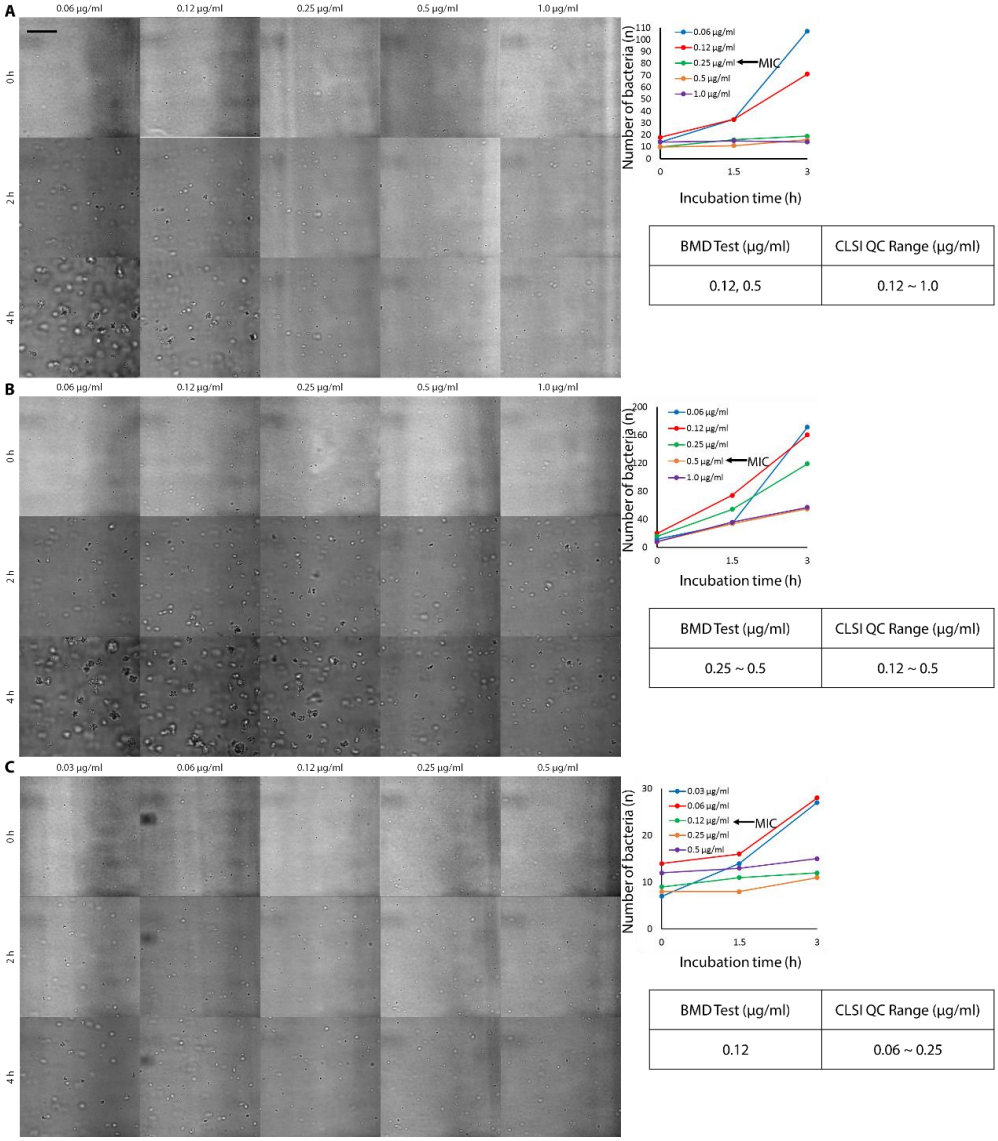

Figure 4.7 MIC determination analyzing bacterial number with *S. aureus* ATCC 29213. (A) In the case of gentamicin. At concentration lower than 0.25 μg/ml, bacterial cells divided. However, at concentration equal to or higher than 0.25 μg/ml, the bacterial cells stopped growing. 1.0 μg/ml was determined as the MIC value and

the MIC value was within the CLSI QC range (0.5-2 μg/ml). (B) In the case of ciprofloxacin. The bacterial cells grew fast and divided even at concentration equal to or higher 0.25 μg/ml in 2 hours, but did not divide anymore in 4 hours; whereas bacteria cells continually divided at concentrations lower than 0.25 μg/ml in 4 hours. (C) In the case of clindamycin. Even at concentration lower than 0.25 μg/ml, the bacterial cells divided slowly, but there was a substantial difference in the growth rate between concentrations lower than 0.12 μg/ml and concentrations equal to or higher 0.12 μg/ml. The MIC was determined as 0.12 μg/ml by comparing the relative cell growth. Scale bar, 50 μm [35].

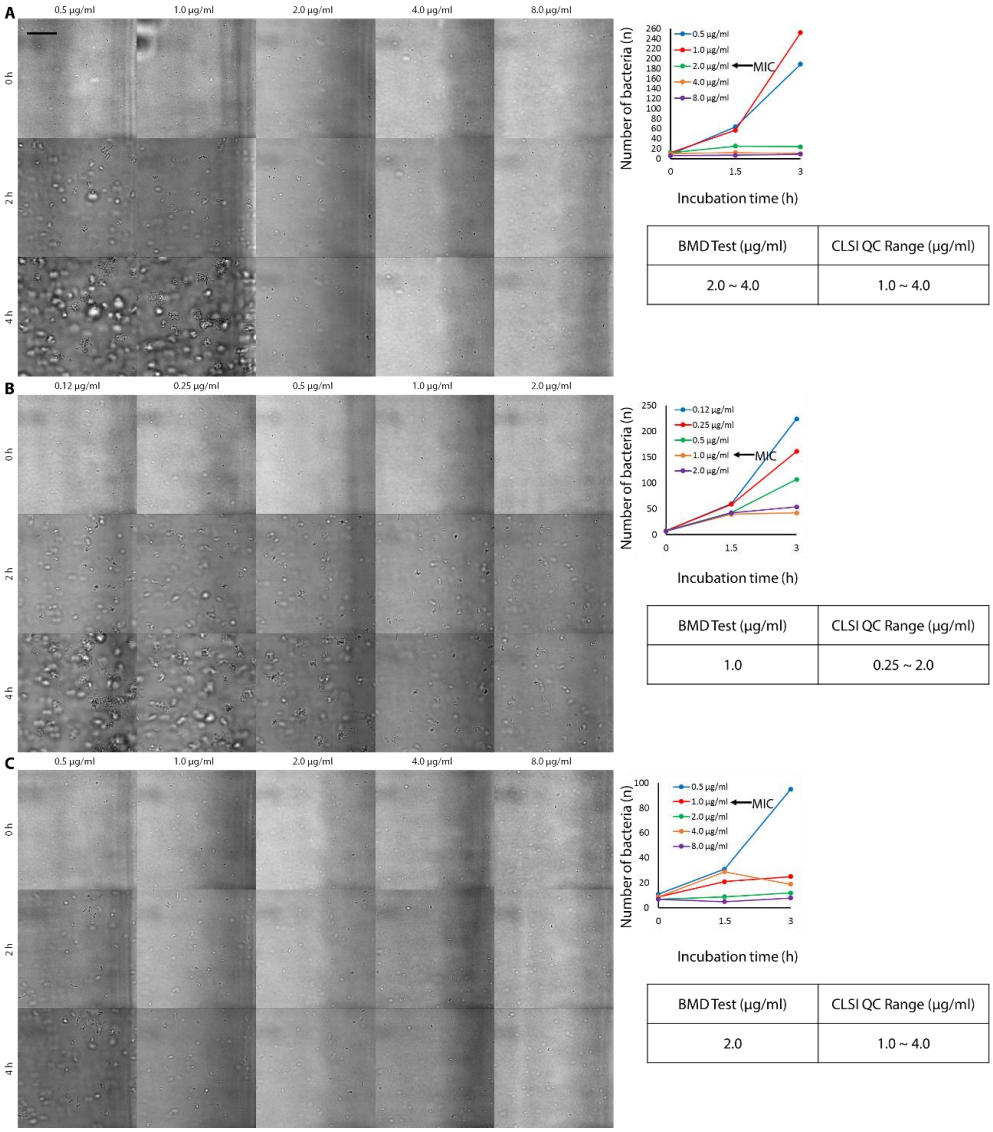

BMD Test (μg/ml)	CLSI QC Range (μg/ml)
2.0 ~ 4.0	1.0 ~ 4.0

BMD Test (μg/ml)	CLSI QC Range (μg/ml)
1.0	0.25 ~ 2.0

BMD Test (μg/ml)	CLSI QC Range (μg/ml)
2.0	1.0 ~ 4.0

Figure 4.8 MIC determination analyzing bacterial number with *E. faecalis* ATCC 29212. (A) In the cases of vancomycin. (B) In the cases of levofloxacin. In the case of levofloxacin, the bacterial cells grew fast and divided even at concentration equal to or higher 1.0 μg/ml in 2 hours, but did not divided anymore in 4 hours, whereas

bacteria cells continually divided at concentration lower than 1.0 μg/ml in 4 hours. (C) In the case of linezolid. Even at concentrations lower than 1.0 μg/ml, the bacterial cells divided slowly, but there was a difference in the growth rate between concentrations lower than 1.0 μg/ml and at concentrations equal to or higher 1.0 μg/ml. The MIC in (B) and (C) was determined by comparing the relative cell growth. Scale bar, 50 μm [35].

Table 4.3 Morphological characteristics of *E. coli* ATCC 25922 in response to different antimicrobial agents. Drugs were administered at a concentration equal to or higher than the MIC. The criteria for bacterial response to a given drug were applied after 3 hours. Antimicrobial susceptibility was determined using the BMD test results and the quality control ranges from CLSI [35].

Antibiotic	**Morphological changes at or over MIC**	**Category**	**Antimicrobial class**
Amikacin	None	Non-β-lactams	Aminoglycosides
Amoxicillin/ clavulanic acid	Swelling	β-Lactams	Penicillins/β-lactamase inhibitor
Ampicillin	Filament	β-Lactams	Penicillins
Aztreonam	Filament	β-Lactams	Monobactams
Cefazolin	Filament	β-Lactams	Cephems
Cefepime	Filament	β-Lactams	Cephems
Cefotaxime	Filament	β-Lactams	Cephems
Cefoxitin	Filament	β-Lactams	Cephems
Ceftazidime	Filament	β-Lactams	Cephems
Ciprofloxacin	None	Non-β-lactams	Fluoroquinolone
Gentamicin	None	Non-β-lactams	Aminoglycosides
Imipenem	Swelling	β-Lactams	Penems
Norfloxacin	None	Non-β-lactams	Quinolones
Piperacillin	Filament	β-Lactams	Penicillins
Piperacillin/ tazobactam	Filament	β-Lactams	Penicillins/β-lactamase inhibitor
Tetracycline	None	Non-β-lactams	Tetracyclines
Trimethoprim/ sulfamethoxazole	None	Non-β-lactams	Folate pathway inhibitors

Table 4.4 Morphological characteristics of *P. aeruginosa* ATCC 27853 for different antimicrobial agents. The criteria for bacterial response to a given drug is described. The criteria for bacterial response were applied after three hours in the MAC. The antimicrobial susceptibility was determined using the BMD test results and the quality control ranges from CLSI [35].

Antibiotic	**Morphological changes at or over MIC**	**Category**	**Antimicrobial class**
Amikacin	None	Non-β-lactams	Aminoglycosides
Aztreonam	Filament	β-Lactams	Monobactams
Cefepime	Filament	β-lactams	Cephems
Cefotaxime	Filament	β-lactams	Cephems
Ceftazidime	Filament	β-lactams	Cephems
Ciprofloxacin	None	Non-β-lactams	Fluoroquinolones
Gentamicin	None	Non-β-lactams	Aminoglycosides
Imipenem	Swelling	β-lactams	Penems
Meropenem	Swelling	β-lactams	Penems
Piperacillin	Filament	β-lactams	Penicillins
Piperacillin/ Tazobactam	Filament	β-lactams	Penicillins/β-lactamase inhibitor
Ticarcilin	Filament	β-lactams	Penicillins
Ticarcillin/ Clavulanic acid	Filament	β-lactams	Penicillins/β-lactamase inhibitor
Tobramycin	None	Non-β-lactams	Aminoglycosides

Table 4.5 Morphological characteristics of *S. aureus* ATCC 29213 for different antimicrobial agents. The criteria for bacterial response to were applied after four hours in the MAC. The antimicrobial susceptibility was determined using the BMD test results and the quality control ranges from CLSI. RRG, relatively rapid growth; RSG, relatively slow growth [35].

Antibiotic	**Criteria**	**Category**	**Antimicrobial class**
Ampicillin	Normal	β-Lactams	Penicillins
Amoxicillin/ clavulanic acid	Normal	β-lactams	Penicillins/β-lactamase inhibitor
Ciprofloxacin	RRG	Non-β-lactams	Fluoroquinolones
Clindamycin	RSG	Non-β-lactams	Lincosamides
erythromycin	RSG	Non-β-lactams	Macrolides
Gentamicin	Normal	Non-β-lactams	Aminoglycosides
Imipenem	Normal	β-lactams	Penems
Levofloxacin	RRG	Non-β-lactams	Quinolones
Linezolid	RSG	Non-β-lactams	Oxazolidinones
Oxacillin	RRG	β-lactams	Penicillins
Penicillin	Normal	β-lactams	Penicillins
Rifampin	RSG	Non-β-lactams	Ansamycins
Tetracycline	Normal	Non-β-lactams	Tetracyclines
Trimethoprim/ sulfamethoxazole	RRG	Non-β-lactams	Folate pathway inhibitors
Vancomycin	Normal	Non-β-lactams	Glycopeptides

Table 4.6 Morphological characteristics of *E. faecalis* ATCC 29212 for different antimicrobial agents. The criteria for bacterial response were applied after four hours in the MAC. The antimicrobial susceptibility was determined using the BMD test results and the quality control ranges from CLSI. RRG, relatively rapid growth; RSG, relatively slow growth [35].

Antibiotic	**Criteria**	**Category**	**Antimicrobial class**
Ampicillin	Normal	β-Lactams	Penicillins
Ciprofloxacin	RRG	Non-β-lactams	Fluoroquinolones
erythromycin	RSG	Non-β-lactams	Macrolides
Gentamicin High Level	Normal	Non-β-lactams	Aminoglycosides
Levofloxacin	RRG	Non-β-lactams	Quinolones
Linezolid	RSG	Non-β-lactams	Oxazolidinones
Norfloxacin	RRG	Non-β-lactams	Quinolones
Penicillin	Normal	β-Lactams	Penicillins
Rifampin	RSG	Non-β-lactams	Ansamycins
Streptomycin High Level	Normal	Non-β-lactams	Aminoglycosides
Teicoplanin	Normal	Non-β-lactams	Glycopeptides
Tetracycline	RSG	Non-β-lactams	Tetracyclines
Vancomycin	Normal	Non-β-lactams	Glycopeptides

Table 4.7 Accurate MIC determination for the four CLSI standard strains using single-cell morphological analysis (SCMA). For validation of the SCMA, four standard bacterial strains were tested against antimicrobial agents that are commonly used in clinical areas: Gram-negative *E. coli* ATCC 25922 and *P. aeruginosa* ATCC 27853 (A); Gram-positive *S. aureus* ATCC 29213 and *E. faecalis* ATCC 29212 (B). The MIC values were determined using SCMA after time-lapse imaging. The MIC values of SCMA were compared with the MIC ranges (quality control ranges) provided by CLSI. Each test was performed in triplicate unless otherwise noted with an asterisk (*, performed twice). [a] Time to result for SCMA with *S. aureus* was 6 h. [b] Time to result for SCMA with *E. faecalis* was 6 h [35].

Antimicrobial (μg/ml)	**MIC, SCMA**	**MIC, BMD**	**CLSI QC range**	**SCMA results**	**BMD Results**	**CLSI QC range**
	(**A**) Gram-negative strains					
	E. coli ATCC 25922			*P. aeruginosa* ATCC 27853		
Amikacin	0.5~1	1~4	0.5~4	1~2	2~4	1~4
Amoxicillin/ clavulanic acid	4/2	4/2	2/1~8/4	-	-	-
Ampicillin	2~4	4	2~8	-	-	-
Aztreonam	0.12	0.12~0.25	0.06~0.25	2~4	4	2~8
Cefazolin	2	2	1~4	-	-	-
Cefepime	0.03~0.06	0.06	0.015~0.12	0.5~2	2	0.5~4
Cefotaxime	0.06	4~8	0.03~0.12	16	16	8~32
Cefoxitin	2	2~4	2~8	-	-	-
Ceftazidime	0.5	0.25~0.5	0.06~0.5	2~4	2~4	1~4

Ciprofloxacin	0.004~0.008	0.008	0.004~0.015	0.25~0.5	0.25	0.25~1
Gentamicin	z0.25	0.25~0.5	0.25~1	0.5~1	1	0.5~2
Imipenem	0.12	0.12	0.06~0.25	1	2~4	1~4
Norfloxacin	0.03~0.06	0.03~0.06	0.03~0.12	-	-	-
Meropenem	-	-	-	1	1*	0.25~1
Piperacillin	2	4	1~4	4~8	8	1~8
Piperacillin/ tazobactam	1/4~2/4	2/4~4/4	1/4~4/4	2/4~8/4	8/4	1/4~8/4
Tetracycline	1	1	0.5~2	-	-	-
Trimethoprim/ sulfamethoxazole	≤0.5/9.5	≤0.5/9.5	≤0.5/9.5	-	-	-
Ticarcilin	-	-	-	16	16	8~32
Ticarcillin/ clavulanic acid	-	-	-	16/2	16/2~23/2	8/2~32/2
Tobramycin	-	-	-	0.25~0.5	0.5	0.25~1
Time to result (h)	3	16~20	16~20	3	16~20	16~20
	(**B**) Gram-positive strains					
	S. aureus ATCC 29213			*E. faecalis* ATCC 29212		
Ampicillin	1	1	0.5~2	0.5~1	0.5	0.5~2
Amoxicillin/ clavulanic acid	0.25/0.12~ 0.5/0.25	0.25/0.12~ 0.5/0.25	0.12/0.06~ 0.5/0.25	-	-	-
Ciprofloxacin	0.5	0.25~0.5	0.12~0.5	0.5~2	1~2	0.25~2
Clindamycin	0.12	0.12	0.06~0.25	-	-	-
Erythromycin	0.25	0.25~0.5	0.25~1	0.5*	2~4	1~4
Gentamicin	0.25~0.5*	0.12,0.5	0.12~1	≤500	≤500	≤500
Imipenem	0.03	0.015	0.015~0.06	-	-	-
Levofloxacin	0.12~0.25	0.12~0.25	0.06~0.5	1	1	0.25~2
Linezolid	1~4	2~4	1~4	1~2	2	1~4

Oxacillin	0.5	0.25	0.12~0.5	-	-	-
Norfloxacin	-	-	-	2~4	2~4	2~8
Penicillin	0.5	1	0.25~2	1~2	1~2	1~4
Rifampin[a]	0.004~0.008	0.004~ 0.008*	0.004~ 0.015	0.5	0.5	0.5~4
Streptomycin high level	-	-	-	≤500	≤500	≤500
Teicoplanin	-	-	-	0.5	0.25~0.5	0.25~1
Tetracycline[b]	0.12~0.5	0.12,0.5	0.12~1	8	8~16	8~32
Trimethoprim/ sulfamethoxazole	≤0.5/9.5	≤0.5/9.5	≤0.5/9.5	-	-	-
Vancomycin	1	1	0.5~2	2~4	2~4	1~4
Time to result (h)	4	16~20	16~20	4	16~20	16~20

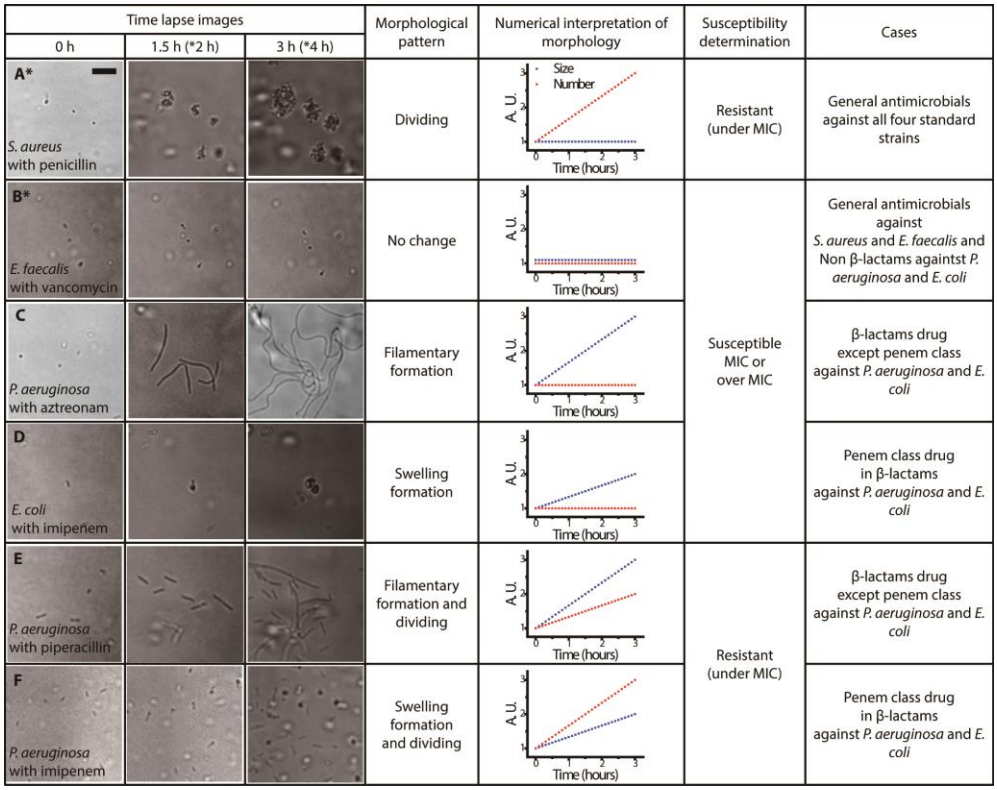

Figure 4.9 Morphological categorization of single cells against antibiotics. After time-lapse imaging of the single bacterial cells, their growth patterns against the antibiotics were analyzed and classified into four groups. (A) Typical division in the antibiotic-free or the antibiotic-resistant conditions, in which bacterial cells divide into two cells. (B) Typical antibiotic-susceptible conditions, in which bacteria do not grow. (C) Filamentary formation conditions for Gram-negative strains in response to β-lactam antibiotics, in which the bacterial cells show filamentary growth, but do not divide. (D) Swelling formation conditions for Gram-negative strains in response to imipenem and meropenem, in which the bacterial cells are swollen but do not divide.

Cases (C) and (D) were considered to be “susceptible”. (E) Co-existence of filamentary formation and dividing. (F) Co-existence of swelling formation and dividing. Cases of (E) and (F) were considered as “resistant”. *For Gram-positive strains, the time-lapse images were taken at 0, 2 and 4 hrs. Scale bar, 20 μm [35].

4.2.2 Automated susceptibility determination based on SCMA

Determination of bacterial susceptibility to antimicrobials based on morphological assessment by a human examiner could be subject to human error. We therefore developed an automated image-processing and classification program to automatically determine susceptibility of various bacterial strains against different antimicrobial agents. Figure 4 shows the schematic representation of our automated analysis. To determine the six morphological patterns (in Fig. 4.10), the total areal occupancy of cells (A_i), the number of bacterial cells (F_i), and the total length of bacteria cells (L_i) were automatically evaluated from each time-lapsed image. Details of the image processing, such as digital filtering, binary conversion, and line detection, are explained in Figs. 4.11 and 4.12 and Table 4.8.

In the cases of Gram-positive bacteria, there are only two morphological patterns: the dividing case (resistant) and the “no change” case (susceptible). For no-change cases, the change in area only needs to be examined. When area increased to a certain threshold rate, it was determined to be resistant (Fig. 4.10A).

In the cases of Gram-negative bacteria, there are six morphological patterns: the dividing case (resistant), no-change case (susceptible), filamentary formation (susceptible), and swelling formation (susceptible), co-existence of filamentary formation and dividing (resistant) or swelling formation and dividing (resistant). For Gram-negative bacteria, all parameters—area, number of cells, and length of cells—needed to be evaluated (Fig. 4.10B). Although area may have been increasing, it may have been due to an increase in length; therefore, the case would not be 'resistant' but 'susceptible'.

To determine the threshold values, we examined each raw image from the CCD camera and suggested the thresholds (T_1-T_6) for the ratio between the areas of bacteria (A) and the ratio between the length (L) and number (F) of filament-shaped bacteria (T_7) to match the susceptibility results from human inspection (Fig. 4.10A and 4.10B). The proposed threshold values were refined by comparing the results from human inspection with the results from our image processing program.

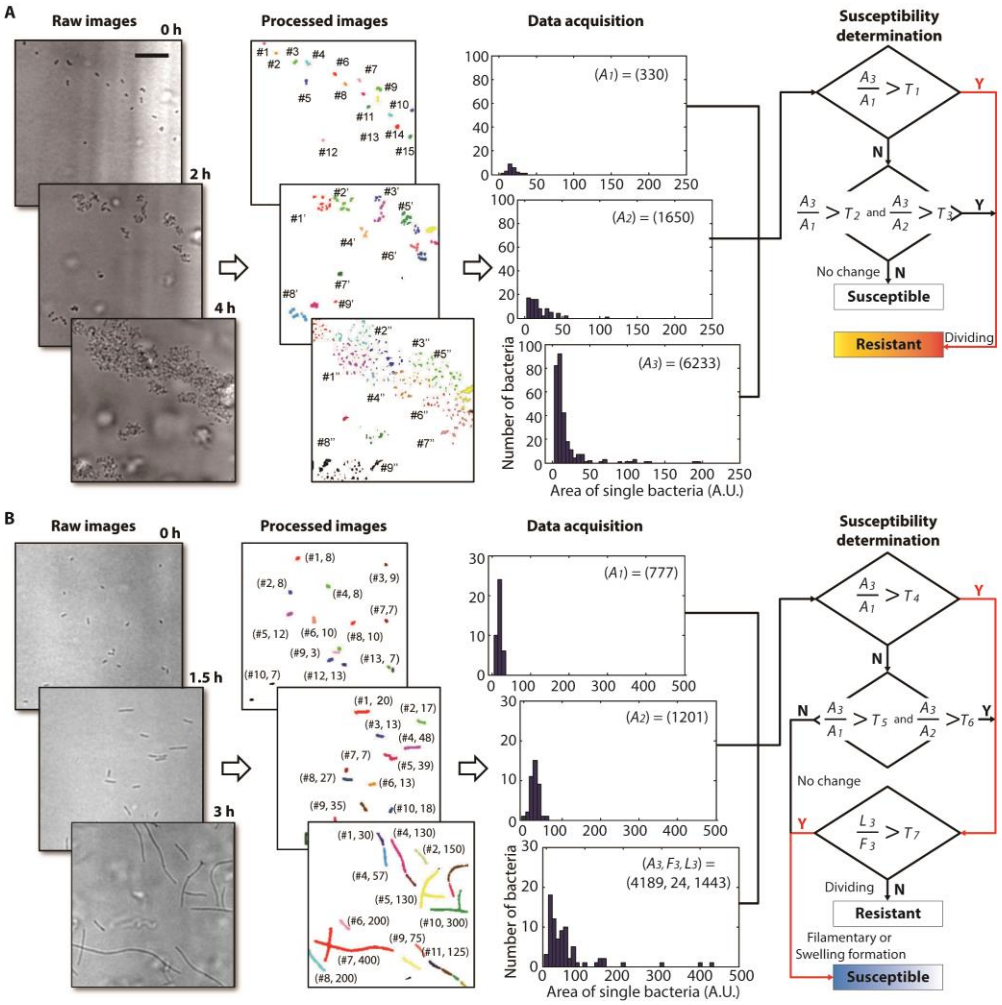

Figure 4.10 Automated image processing and data interpretation. (A) In the case of Gram-positive strains, the raw images were transformed to binary format image by several image-processing algorithms. From the processed images, the data of total area occupancy of cells (A_i) were obtained. The value of bacterial occupancy area in third and final image at 4 hours (A_3) was divided by those of first image at 0 hours (A_1) and the calculated value was compared with the first threshold value (T_1). If

A_3/A_1 was larger than T_1, the case was determined as “resistant”. If the value was smaller than T_1, the second thresholding processes comparing with the second (T_2) and third (T_3) thresholds were performed to determine susceptibility. Two calculated values from A_3/A_1 and A_3/A_2 (A_2, the second image at 2 hours) were compared with T_2 and T_3, respectively. If both values were larger than T_2 and T_3, respectively, then the case was determined as “resistant”. If not, it was “susceptible”. (B) In the cases of Gram-negative strains, the process was same as that of the Gram-positive strain in (A) case except an additional check of abnormal growth (filamentary formation or swelling). All cases with increased area of bacterial cells compared with the threshold values (T_4, T_5 and T_6) were sent to filament and swelling checks. Total length of bacterial cells (L_3) was divided by the number of bacterial cells (F_3), and the calculated value was compared with T_7. If the value was larger than T_7—implying filamentary formation or swelling—the case was determined as “susceptible”. If not larger, it was regarded as “resistant”, implying a dividing case. A_1, A_2 and A_3 are the values of bacterial growth area according to incubation times (0, 2, and 4 hours for Gram-positive strains and 0, 1.5, and 3 hours for Gram-negative strains). T_1, T_2, T_3, T_4, T_5, T_6 and T_7 are the threshold values determined individually for each strain with different growth rates under various antimicrobial agent conditions. Scale bar, 20 μm [35].

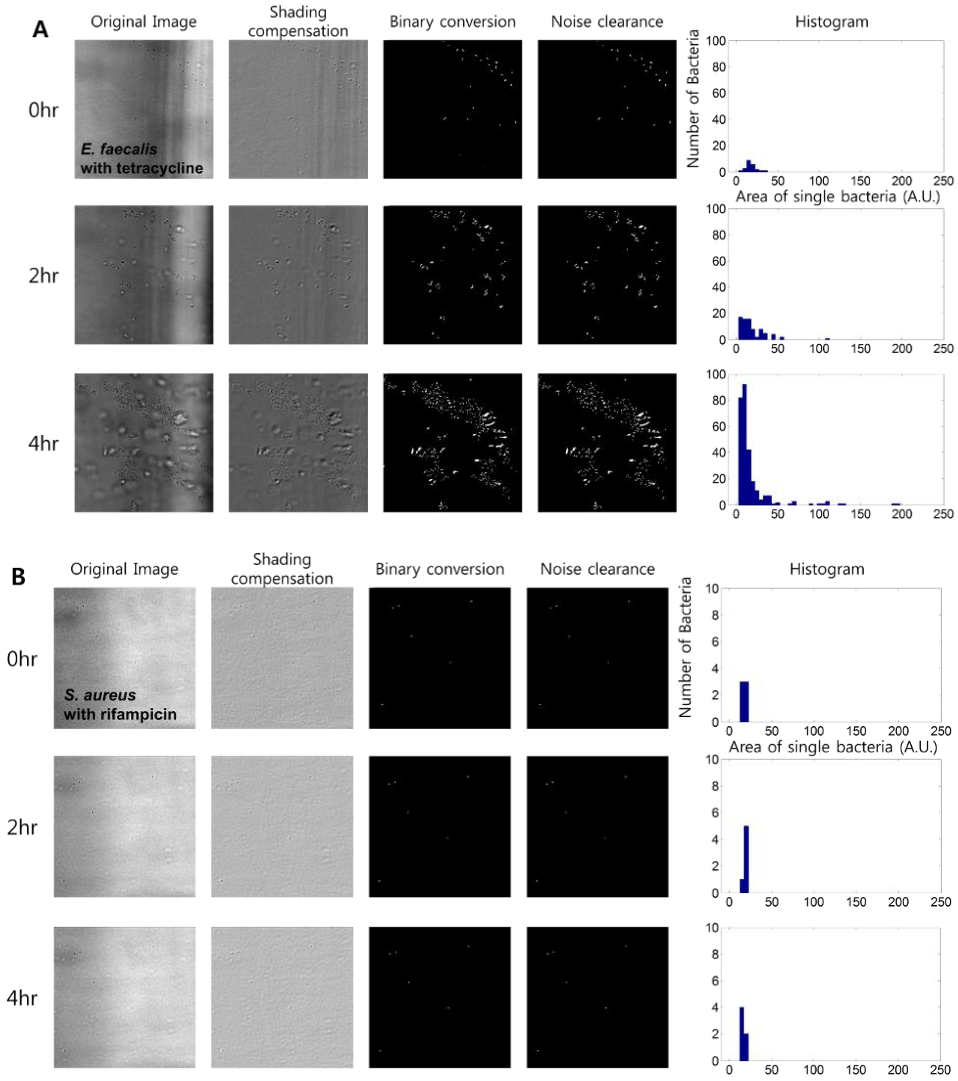

Figure 4.11 Automated image processing for representative Gram-positive strains. Images represent output at each step. Details of how to perform each step are provided in table S6. (A and B) Gram-positive strains: *E. faecalis* treated with tetracycline (A) and *S. aureus* treated with rifampicin (B). First step was shading compensation, followed by adaptive filtering and binary conversion, and noise

elimination and borderline clearance. Data were acquired as histograms showing the number of bacteria in bins of “area” (number of pixels occupied) of a single bacterium [35].

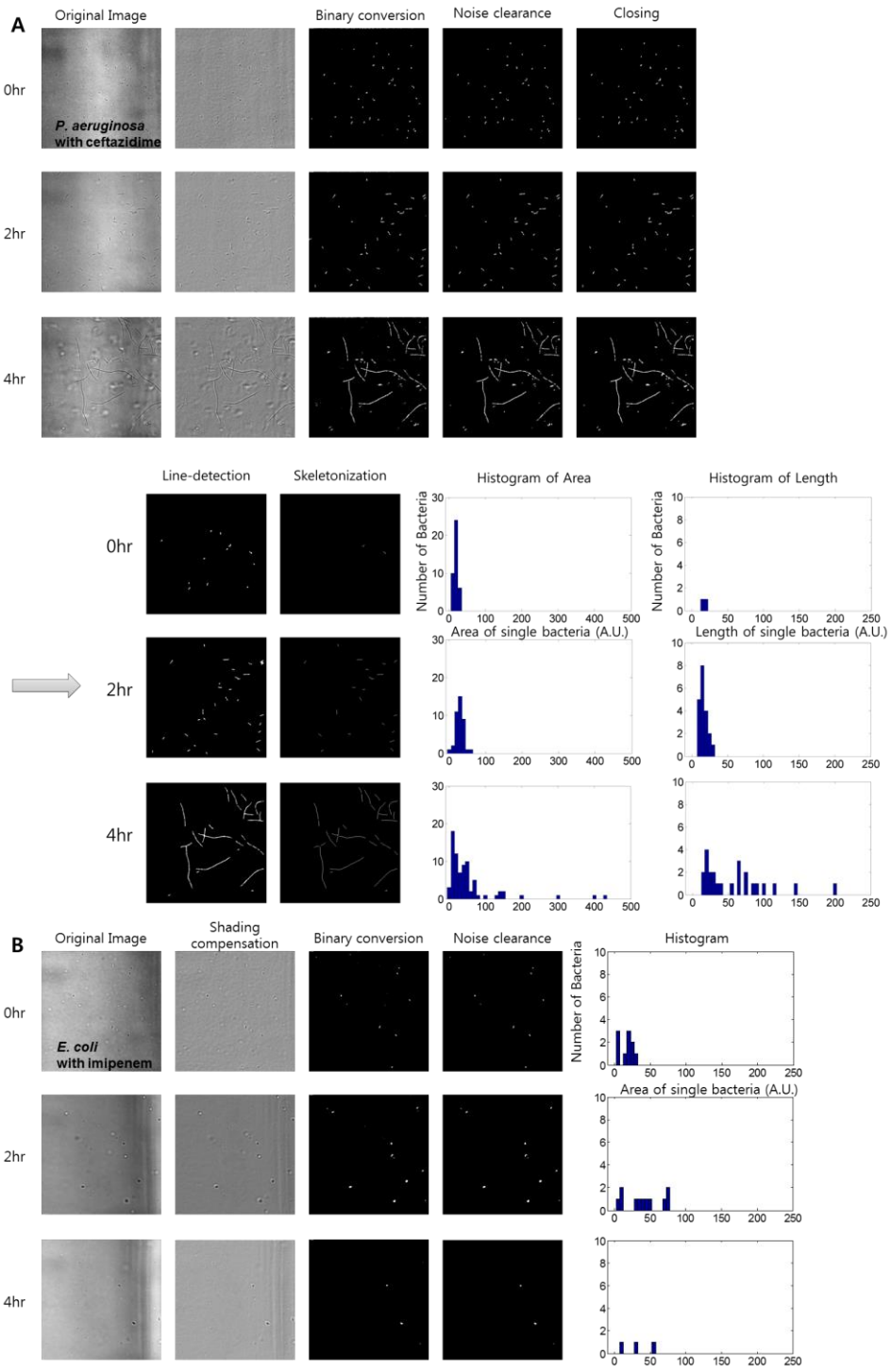
A
Original Image
Binary conversion
Noise clearance
Closing
0hr
2hr
4hr
P. aeruginosa
with ceftazidime
Line-detection
Skeletonization
Histogram of Area
Histogram of Length
Number of Bacteria
Area of single bacteria (A.U.)
Length of single bacteria (A.U.)
B
Original Image
Shading compensation
Binary conversion
Noise clearance
Histogram
E. coli
with imipenem

Figure 4.12 Automated image processing for representative Gram-negative strains. Images represent output at each step. Details of how to perform each step are provided in Table 4.8 (A and B) Gram-negative strains: *P. aeruginosa* treated with ceftazidime (A) and *E. coli* treated with imipenem (B). Images were obtained and processed similar to Gram-positive bacteria with shading compensation, adaptive filtering and binary conversion, and noise elimination and borderline clearance. However, Gram-negative bacteria with filamentary formation owing to β-lactam drugs in (A) [except the penem class in (B)] also required the following steps described in table S6: closing, line detection preparation, line detection, thinning, skeletonization, and data acquisition [35].

Table 4.8 Explanation of the image-processing algorithm. Briefly, the raw images were first processed to remove noise and obtain binary-format images representing only the background and the bacterial features. Information about the bacterial cells in the images, such as area, number, and length, was acquired by calculating the pixel information of bacterial features in the images [35].

Process	**Detailed explanation**
Shading compensation	The raw image had uneven brightness caused by the focusing effect of the poly(methyl methacrylate) (PMMA) chip. To moderate this unevenness, shading compensation was performed. 1) The image (512 x 512 pixels) was divided into segment of $n \times n$ pixels. The value of each segment was calculated, and the average value was obtained. 2) Segments with brightness >1 SD away from the average were compensated by their difference from the average. 3) As a result, all of the segments had uniform brightness. In this experiment, n=10.
Adaptive filtering and binary conversion	Images were divided into 20 x 20 pixels sized segments. For each segment, local average of pixel values was calculated and pixels whose values were lower than '0.75 x local average' were segmented. The weighting value 0.75 was empirically selected

	through comparison of segmentation results obtained using various weighting values ranging from 0 to 1.
Noise elimination and borderline clearance	Lumps smaller than bacterial cells were regarded as artifacts and eliminated. The artifacts at the border line of the image were also eliminated.
Closing	In the case of filamentary formations, to detect lines effectively, finely separated lines were reconnected.
Line detection preparation	Lumps with no line shape were removed for line detection. 1) An $n \times n$ matrix segment was generated in the image and traced to determine whether it contained any elements with a value of '1'. 2) If so, the elements with value "1" were changed to value '0'. For example, when we considered two 3×3 matrices (red shading, yellow box), the left panel had both '0' and '1' value in the matrix, while the right panel had value '1' in all elements in the matrix. In the right panel, the elements of the matrix were all changed to '0'. As a result, the lump pixels were removed and small segments remained.

	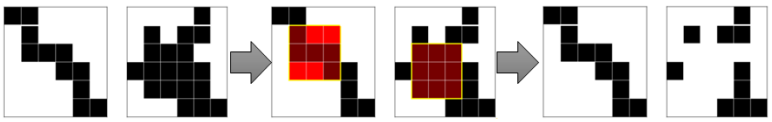
Line detection	The small lumps remaining from the line detection preparation process were eliminated, and the finely separated lines were re-connected.
Thinning and skeletonization	To measure the length of the line, the image was processed by thinning and skeletonization. After skeletonization, unless two lines intersected, each non-zero pixel was adjacent to only one other non-zero pixel.
Data acquisition	For the Gram-positive cases, the total number of non-zero pixels in the image was calculated. For the Gram-negative cases, the line length was measured by tracing the non-zero pixels in a line. Lines were traced one at a time. If the distance between two lines was less than 10 pixels, the two lines were counted as one line. In the case of an intersection, two lines crossed. The number of lines in the image was added up to produce the correct total number of lines. 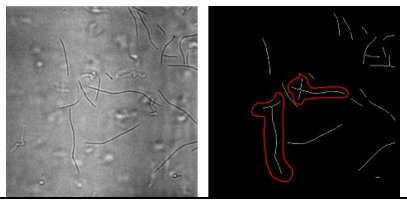

4.2.3 SCMA for determination of antimicrobial susceptibility in clinical samples

We tested 189 clinical isolates (42 *E. coli*, 34 *P. aeruginosa*, 30 *K. pneumoniae*, 45 *S. aureus*, and 38 *Enterococcus* spp.) (Fig. 4.13A). Clinical strains from various specimens (blood cultures, wound specimens, and urine) were collected from the labs of Seoul National University Hospital (SNUH, 149 strains) and Incheon St. Mary's Hospital (ISMH, 40 strains). The collection included various phenotypes with special resistance mechanisms: 37 extended spectrum beta-lactamase (ESBL)–producing *Enterobacteriaceae* spp., 17 imipenem-resistant *Pseudomonas aeruginosa* (IRPA), 24 methicillin-resistant *Staphylococcus aureus* (MRSA), and 16 vancomycin-resistant *Enterococci* (VRE). The clinical bacterial samples were prepared on either sheep blood agar or Mueller Hinton Agar (MHA) plates. Prior to testing, each isolate was subcultured on cation-adjusted MHA for 20–24 hours. Our ASTs using SCMA were performed in the MACs simultaneously with the gold standard BMD test as reference AST.

To produce discrepancy rates, the AST results from SCMA were compared with the results from the BMD test (Fig. 4.13B). To examine the accuracy of our clinical interpretations, category agreement, minor errors (mE), major errors (ME), and very major errors (VME) were calculated, as defined by the FDA guidance document for each organism [42]. The total category agreement for all isolates was 91.5% and the minor error rates, major error rates, and very major error rates were

6.51, 2.56, and 1.49%, respectively, for SCMA (Fig. 4.13B). The SCMA AST took only 3-4 hours and required only 10-20 bacteria in a single image (200 μm × 200 μm) to produce AST results and the error and categorical agreement rates satisfied the FDA requirements for AST systems (mE ≤ 10%, ME ≤ 3.0%, VME ≤ 1.5%, CA ≥ 90%).

Overall, the AST results for Gram-positive strain indicated higher category agreement rates and lower error rates compared to Gram-negative strains (Fig. 4.13B). In the Gram-negative strains, β-lactam antimicrobial agents produced lower category agreement rates than non–β-lactam antimicrobial agents because filamentary or swelling formations induced by β-lactam antimicrobials increased the error rates of the SCMA method compared with dividing or non- dividing cases under non–β-lactam antimicrobial agents (Fig. 4.13C). For *P. aeruginosa*, the lowest category agreement rate was for β-lactam antimicrobial treatment. In the Gram-positive strains, there were no significant differences between β-lactam and non–β-lactam antimicrobial agents because there were no morphological differences between them.

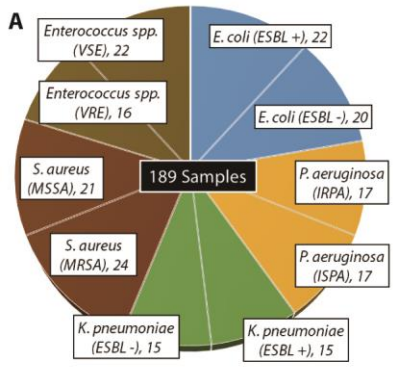

B **Strain name, number of samples**

Bacteria	n Tests	BMD test			Discrepancy number			Discrepancy rate (%)				Average TTR (h)
		S	I	R	mE	ME	VME	mE	ME	VME	CA	
Gram negative	1423	862	85	478	117	26	9	8.15	3.25	1.88	89.3	3
Gram positive	975	547	31	397	39	10	4	4.00	1.82	1.01	94.6	4
Total	2398	1409	116	875	156	36	13	6.51	2.56	1.49	91.5	3~4

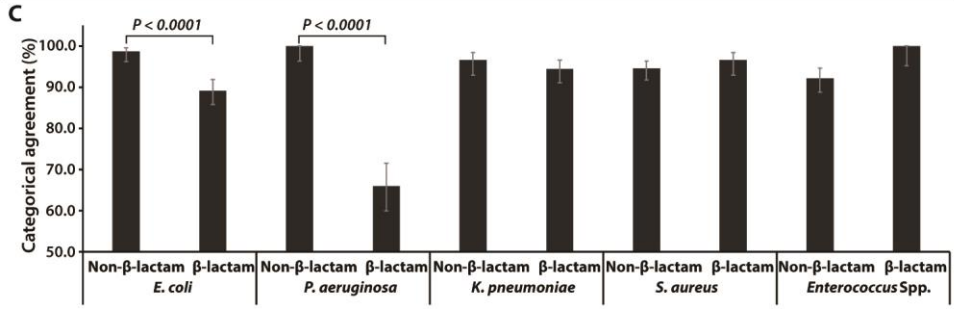

Figure 4.13 Discrepancy rates and categorical agreement rates for SCMA using clinical samples. (A) Distribution of the 189 clinical samples from SNUH and ISMH. (B and C) The SCMA AST results were compared with the clinical gold standard BMD test. Discrepancy rate and categorical (CA) agreement rates were calculated. (B) Summary of the discrepancy and CA rates. Total values were calculated with all AST results from Gram-positive and -negative cases. For BMD test: S, susceptible; I, intermediate; R, resistant. For the SCMA: mE, minor error;

ME, major error; VME, very major error. TTR, time to results. (C) CA rates according to the different clinical strains in response to β-lactam and non–β-lactam antimicrobial agents. Error bars represent 95% confidence intervals determined by Wilson's binomial method. *P*-values were determined using a chi-squared test [35].

4.2.4 SCMA reduces AST error rates compared with the bacterial area measuring (BAM) method

SCMA reduced error rates compared with the previous bacterial area measuring (BAM) method [8] for both β-lactam and non–β-lactam antibiotics against Gram-negative strains *E. coli*, *P. aeruginosa*, and *K. pneumoniae* (Fig. 4.14). For the β-lactam antimicrobial agents, the major error rates were dramatically reduced (from 12.8% to 0.9% for *E. coli* and 48.1% to 13.7% for *P. aeruginosa*). The minor error rates were slightly reduced (from 10.3% to 9.7% for *E. coli* and 6.7% to 4.1% for *K. pneumoniae*).

Filamentary responses of Gram-negative strains to *β*-lactam antimicrobials were determined "resistant" by the BAM method, which only considers the change in bacterial area. However, the cases were deemed "susceptible" by the BMD test, resulting in a high major error rate. Using our SCMA, the filament cases were determined to be susceptible, in agreement with the BMD test, thus reducing the major error rates. In addition, the SCMA significantly reduced the major error rates for non–*β*-lactam antimicrobial cases in *E. coli*. The SCMA slightly reduced the minor error rates in the other cases because it determined susceptibility by sensing more delicate morphological changes, whereas the bacterial area measuring method recognized only increases in the area of bacterial growth.

In rare cases, there was filamentary growth in SCMA (deemed "susceptible") with increased OD values in the BMD test (deemed "resistant") causing very major

errors: two VME cases out of 390 in *E. coli* and six VME cases out of 253 in *P. aeruginosa*. This could have been caused by the limited imaging area (200 μm × 200 μm). In these cases, we speculate that there was only filamentary formation or swelling formation in the imaged area while cell division co-existed in the other areas.

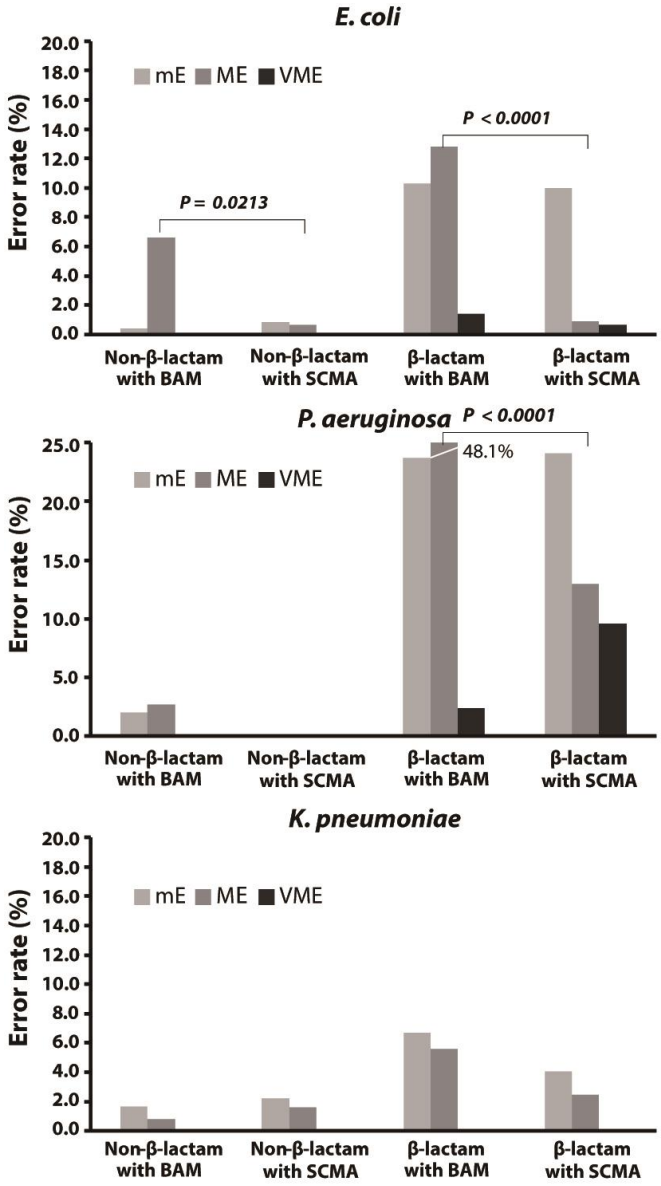

Figure 4.14 SCMA reduces AST error rates compared with the bacterial area measuring (BAM) method. Data are the AST error rates for clinical Gram-negative strains *E. coli* (n=42), *P. aeruginosa* (n=34), and *K. pneumoniae* (n=30) tested with

non–β-lactam and β-lactam antimicrobial agents. The error rates were calculated by comparing AST results from each method with BMD test. *P*-values were determined using a chi-squared test [35].

4.2.5 Discussion

In this study, we assessed four clinical pathogens representing various bacterial infections, including major antibiotic resistant pathogens (ESBL-positive *E. coli* and *K. pneumoniae*, VRE and MRSA). For other strains, there may be morphological patterns that are not described in this study. However, the basic principle that bacteria should divide to exhibit visible growth is constant across all strains, which suggests that SCMA will be broadly applicable.

The MAC system using SCMA produced accurate AST results in only 3-4 hours. The results were compared with the conventional AST, which takes 64-68 hours in total, including the blood culture. In rapid AST with our SCMA system, the total testing time can be reduced to 52 hours, about 25% less than conventional methods, because it detects single cell responses against antimicrobial agents. Considering daily work time (9 hours in average), proper antimicrobial treatments with the

results from conventional AST system can be performed on the following day. However, when performing SCMA in the MAC system, same-day antimicrobial treatments are possible, owing to its shortened test time. Same-day AST in microbiology laboratories can have a major impact on the care and outcome of hospitalized patients with infections that require curative antibiotic treatments [43].

The morphological changes of Gram-negative bacteria in response to β-lactam antibiotics have been studied previously [29, 30]. Penicillin-binding proteins polymerize and modify peptidoglycans (the stress-bearing components of bacterial cell walls), leading to morphological deformations, including filamentary formation and swelling. The relationship between filamentary formation and MIC was observed by Buijs *et al*. [44], but they could not determine a MIC value because filamentary formation occurred over a broad range of antimicrobial concentrations that were variably below, equal to, and above the MIC. In our study, we used automated SCMA to objectively examine morphological changes for MIC determination. Cases of filamentary formation or swelling were regarded as susceptible because the OD value did not increase. This indicated efficient inhibition of the bacterial cells. In some cases, morphological deformation and division matched. These cases were regarded as resistant because some resistant bacterial cells dominated to increase the OD.

Hospital ASTs such as VITEK2 and MicroScan can test approximately 60 combinations of antimicrobial agents at different concentrations. We integrated microfluidic channels with 96-well plates to exclude syringes and tubing systems. In our system, nutrient and antibiotic solution is provided directly from well into the microfludic agarose channel where bacterial cells are immobilized. However, an auto pipetting system is needed to load bacterial cells and nutrient (antibiotic) solution to meet these high-throughput clinical requirements In addition, imaging data–acquisition of SCMA took 20~30 minutes per one test sample which is slower than conventional ASTs based on the turbidity measurement taking less than 1 minute (Vitek 2 and MicroScan). Bright field imaging of an entire 96-well MAC chip with a 60x objective lens will take too much time to be a clinically relevant way of imaging. Instead, we performed single-spot 60x imaging per well (FOV was 200 x 200 μm^2), which was sufficient to obtain a bacterial susceptibility result for that well. Therefore, imaging 60 different combinations in the MAC chip requires 60 different bright field imaging at 60x. Because the imaging location is already known and predetermined by microfluidic chip design, it takes approximately 20 minutes in manual setting and would take less than 5 minutes in automated system. To reduce the time for imaging, finding proper z-location (focusing) is important. We have implemented a high-resolution focusing mark in our microfluidic chip (Fig. 4.2B).

In addition, the MAC system with SCMA can be used to observe morphological

reactions against antimicrobial agents with single-cell resolution, whereas conventional AST systems and many rapid AST systems can only be used to observe bacterial population behavior (susceptible or resistant) [38, 45, 46]. This suggests that the MAC system can provide more information for clinical pathologists and researchers on antibiotic resistance mechanisms. Although not investigated here, this may help improve our understanding of the mode of action of antibiotics.

Bacterial identification with AST result is necessary for accurate prescription of antimicrobials to the bacterial infected patients. In commercialized AST platforms, AST is performed simultaneously with the bacterial identification (ID) assay because effective antibiotic treatments require not only AST results but also bacterial ID. The test time required for bacterial identification is generally shorter than the time for AST. Owing to the fast identification capabilities of mass spectrometry [47], there are some commercial AST platforms that have integrated with this analytical technique, such as the VITEK MS. The MAC system with SCMA could be easily integrated with mass spectrometry–based platforms for bacterial identification, which would supply the best synergy effect for diagnosis.

In this study, the five clinically important strains *E. coli*, *P. aeruginosa*, *K. pneumoniae*, *S. aureus* and *Enterococcus* spp. were tested, and their morphological patterns under various antibiotics were analyzed to establish criteria for SCMA. However, for other clinical strains under certain antibiotic conditions, other

morphological patterns may arise; these SCMA criteria may not be applicable to other patterns. To apply SCMA in clinical settings, more clinical strains need to be tested and their morphological patterns need to be included in the SCMA criteria. Also the three hour AST via SCMA can be perfectly matched with emerging fast bacterial identification method such as mass spectroscopy. Here we trained our SCMA algorithm to match with the BMD method, current clinical golden standard for AST, to demonstrate SCMA meeting the current FDA requirement of accuracy. However, we think SCMA has potential to become better clinical golden standard than BMD since it is can incorporate heterogeneity in bacterial responses to various antibiotics. Most of all, SCMA is more than five times faster than BMD without trading off the accuracy.

In conclusion, the SCMA can determine bacterial susceptibility antimicrobial drugs, faster and more accurately than conventional AST and the gold standard BMD. This technology was validated with clinical samples (MRSA, VRE, IRPA, and ESBL-positive *E. coli* and *K. pneumoniae*), suggesting that it will be suitable for broad clinical use. For clinical translation of rapid AST with SCMA, full automated system with sample preparation, image acquisition and analysis will be needed.

4.3 Summary

In summary, the SCMA can determine bacterial susceptibility antimicrobial drugs, faster and more accurately than conventional AST and the gold standard BMD. This technology was validated with clinical samples (MRSA, VRE, IRPA, and ESBL-positive *E. coli* and *K. pneumoniae*), suggesting that it will be suitable for broad clinical use. For clinical translation of rapid AST with SCMA, full automated system with sample preparation, image acquisition and analysis will be needed.

Chapter 5 Rapid DST of M. tuberculosis by single cell tracking method

In this chapter, I applied a single cell tracking method to reduce the time for DST. *Mycobacterium tuberculosis* (MTB) was inoculated in the agarose matrix used for 3D culture environment and drug delivery. For single cell tracking of MTB cells, we fabricated a microfluidic chip which contains a chamber for cell immobilization and drug delivery. By observing responses of MTB to a drug with single cell resolution using microscopy, we differentiated growth and non-growth of MTB under the TB drugs and their concentrations and determined drug susceptibility only in five days which is concordance with the DST results from conventional method. This rapid DST method can reduce DST time dramatically and be used for fast and accurate treatments for TB patients leading the increase of the cure rate.

5.1 DST process in the disk agarose culture (DAC) system

5.1.1 Design of a chip and its fabrication process

For microscopic time lapse imaging of TB, a test chip is needed to provide the immobilization of TB in agarose for a sufficient delivery of drugs and optical transparency. To satisfy these requirements, a new chip called a Disc Agarose Culture (DAC) chip was designed and fabricated. (Fig. 5.1) The DAC chip is composed of a disc-shape channel where the agarose and TB mixture is are loaded and there are structures for enhancing the diffusion of the culture medium and drugs such as well for containing culture medium, drug, open space and hole. The depth of the disc shape channel is determined by the height of a spacer and its value was 300um. The dimension of the chip is described in Fig 5.1B. For DST of TB, a long time of incubation is necessary and the culture medium should be supplied sufficiently to TB. Using a syringe pump of for supplying the medium is restricted due to an inconvenience issue and limitation of throughput of the system. Therefore, each well is designed in the size of a single well in a 24 well plate. In terms of dimensions, the length and height of the well is are 11mm and 10mm, respectively, and it contains about 1mL of medium which is suitable of for more than 1 month of incubation. Fabrication of chips using PDMS limits the dimensions of the chip, and the manufacturing throughput is low. Therefore, the injection molding is used for

fabricating the DAC chip. After designing the chip using a 3D design tool (SolidWorks), the aluminum mold was machined. Poly(methyl methacrylate) (PMMA) was used for building chips. After the fabrication of chips, polycarbonate film was bonded at the bottom of the chip using the solvent bonding method. The chamber was designed with a 3D design tool and made by utilizing injection molding process. Moreover, the bottom film, polycarbonate is bonded by a solvent ((80:20 in weight, ethanol: 1,2-dichloroethane, Sigma-Aldrich) with pressure. After the bonding of the chip, the O_2 plasma treatment is performed for the hydrophilic treatment. For sterilization, the gamma ray treatment is performed for 5 hours.

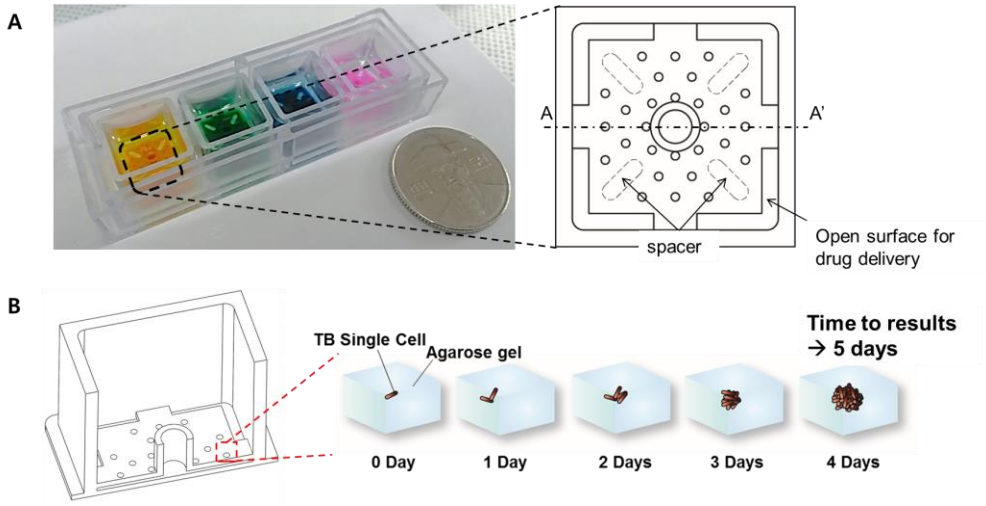

Figure 5.1 A) Poly(methyl methacrylate) (PMMA) chip and its top-view. B) Rapid DST based on microscopic single cell tracking in agarose matrix takes only 4 days to obtain DST results.

5.1.2 DST process

For DST in DAC chip, the chip is treated with O_2 plasma for hydrophilic enhancement and Gamma radiation treatment for sterilization. For preparation of a TB stock solution, the colonies in LJ medium was collected using sterilized loop. The aggregated colonies in an u-shape bottom tube were was dispersed by vortexing with glass bead with 2mm diameter. Due to safety issues, the vortexed tube was stayed for 15 minutes. After the stabilization, 7H9 medium with 10% of OADC is added to prepare the stock solution with McFarland 1.5~3.0. The stock solution was mixed with 0.5% agarose at 37℃ by vortexing. The 40 ul of mixture of TB stock and agarose was loaded into the inlet of DAC chip and the agarose was solidified in the room temperature after 1 minute. The 1ml of TB drugs diluted in 7H9 with 10% OADC is added into the DAC chip. The drug in the culture medium was diffused into the agarose. After this process, the DAC chip is was sealed by air permeable film for preventing the evaporation of the culture medium and incubated in a temperature controlled culture chamber at 37℃. A one area in the edge of the agarose was imaged using the time lapse method in every day with a 40X lens with inverted microscopy. All these processes were processed in clean bench (Fig. 5.2).

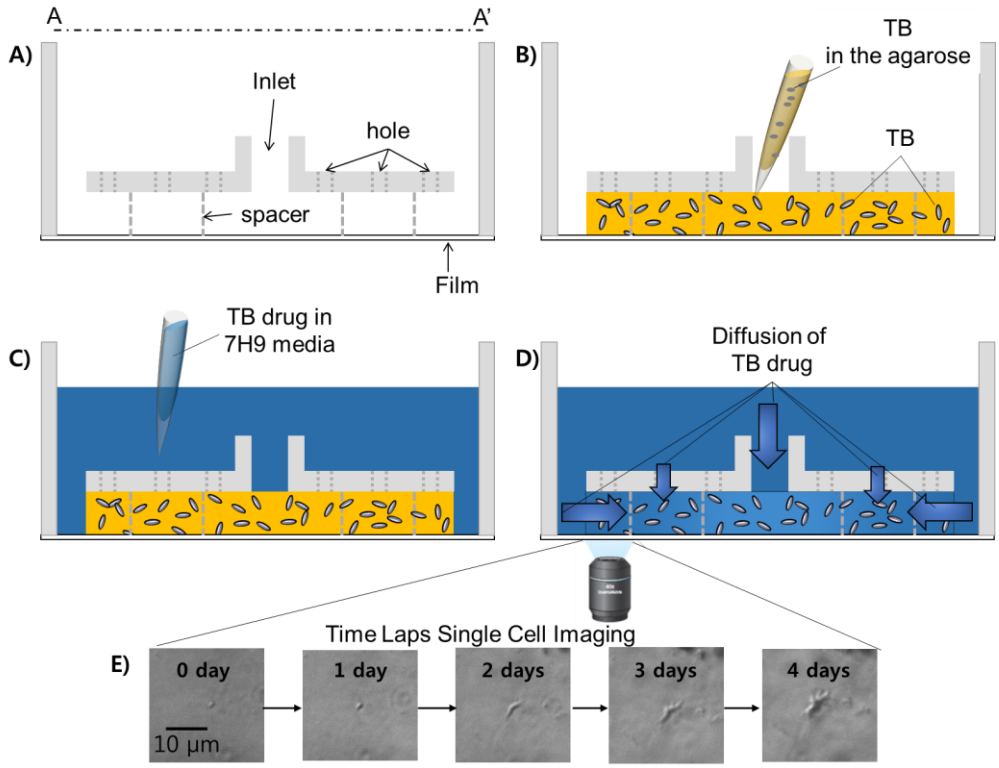

Figure 5.2 Experimental procedure. A) Empty chamber B) Loading MTB cells mixed with agarose at liquid state at 37℃ C) Loading of drug in liquid medium D) Diffusion of drug and culture media and time lapse image to detect the MTB cell growth. E) Time lapse Single cell imaging of standard strain, H37Rv in 7H9 broth media.

5.2 Rapid DST of *M. tuberculosis* using the DAC system

5.2.1 A 3D culture formation chip for the DST of MTB

In this study, agarose was used as a 3D culture matrix for the DST of MTB. For long term incubation for MTB, a stable 3D culture matrix is needed. To verify the stability of agarose matrix, 0.5% agarose was mixed with micro-beads in phosphate buffered saline with 3:1 in volume. The mixture was loaded into the inlet hole in the DAC chip and 7H9 culture media was added in the well. To mimic the DST of MTB condition, the chip was incubated in the 37℃ chamber. The beads in the agarose matrix were observed well at the same place for 3 weeks showing that the 3D culture matrix was stable enough for DST of MTB. When we cultured the H37Rv in the agarose matrix, the structure was also well maintained for single cell tracking for three weeks. To facilitate uniformed supply of liquid culture medium and drug, the agarose matrix was properly formed in the mold. For visualization of formation of the agarose matrix, the 0.5% agarose mixture with food dye at 3:1 in volume was loaded into the chip and imaged (Fig 5.3). The agarose matrix was well formed in the DAC chip.

5.2.2 Diffusion characteristics in the DAC chip

Agarose was used for fixation of the MTB strains. The TB drugs were solved in a liquid medium, 7H9 broth, to be delivered to the MTB strains in the agarose matrix. The diffusion characteristic of agarose have been studied well before [18, 31, 48] . In this research, the uniform concentration of drugs at the imaging area of the corner of the DAC chip imaging area was necessary for accurate DST results. Using the Fick's law, the time (T) for diffusion of molecule to the imaging area (200 x 300 μm from reservoir) was calculated by $T = d^2/2D$, where D is the diffusion constant of a molecule in the media and d is the diffusion distance, respectively. Diffusion coefficient of penicillin (MW : 313 g/mol) in 2% agarose at 37℃ is about 30,000 um^2/min. the diffusion time of the drugs in the imaging area can be about 2 minutes. We used 0.5% agarose which was mixed with the liquid medium. The final concentration is 0.375%, so the diffusion time will be shorter than that in the 2% agarose matrix. Considering the dividing time of MTB is about 20~24 hours, the drug distribution in the agarose matrix can be enough for DST. For visualization of diffusion characteristics of the agarose matrix in the DAC chip, rhodamine B (molecular weight: 479.02 g/mol) was used and its molecular weight is similar to the TB drugs (isoniazid : 137.139, rifampicin : 822.94, streptomycin : 581.574 and ethambutol : 204.31 g/mol). Under 1 ug/ml concentrations of these molecules, the imaging areas were imaged at 0 min, 10 min, 30 min, and 1 hour to measure

diffusion uniformity in Fig 5.3. The fluorescent signal became uniformed only in 30 min after loading of the fluorescent dye implying that there is no problem for DST considering the cell division of MTB take about 20~24 hours. In addition, the growth rate of MTB was mainly even throughout the whole chip area showing that the liquid culture medium and drugs diffused equally into the chip.

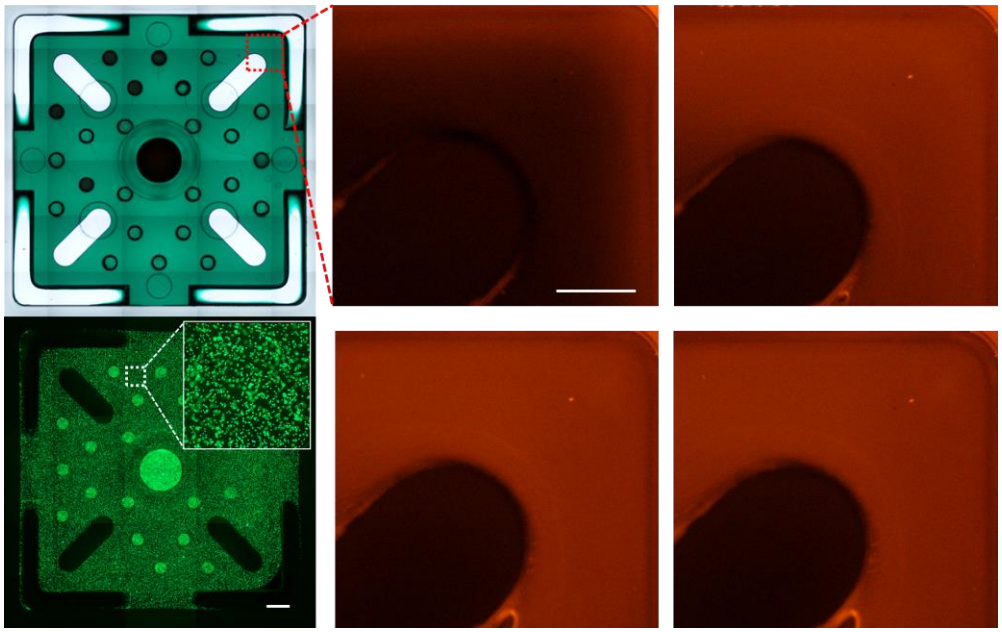

Figure 5.3 Diffusion of antibiotics into agarose. The Image A was taken immediately after rhodamine B was loaded. Images B, C, and D were taken every 10 min in sequence. The dotted boxes show the imaging areas that were used to observe bacterial growth. The exposure time was 0.1 s. The scale bars represent 0.5mm.

5.2.3 Rapid DST using single cell tracking in the DAC system

The MTB DSTs are based on the estimation of growth or no growth of a MTB strain in the presence of single ‘critical concentration’ of one drug. In the common way, the critical concentration of an anti-tuberculosis drug indicates clinically relevant resistance if growth is observed and susceptible TB strains are inhibited by this concentration. In the DAC system, the critical concentration of each anti-tuberculosis drug is decided by reference of MGIT’s critical concentrations because DAC system is might be more similar with the liquid culture system that the solid culture system. After setting up the critical concentration of each anti-tuberculosis drug, DSTs by the DAC system are examined serial two-fold concentration around critical concentration in order to acquire the MIC and susceptibility of *M. tuberculosis*. The MIC values could be acquired because the plenty of anti-tuberculosis drug concentrations were tested. After that, if the MIC values are under the critical concentration, tested strains are susceptible. Otherwise, tested strains are resistance as the MIC values are over the critical concentration. In the case of rifampin, DST by the DAC system was performed at 0.25, 0.5, 1.0, and 2.0 μg/ml concentration from 1.0 μg/ml critical concentration and then a growth curve was generated from each anti- tuberculosis drug concentration according to the incubation time. The susceptibility was decided by measuring the MIC value according to the criteria of critical concentration (Fig 5.4 and Fig 5.5).

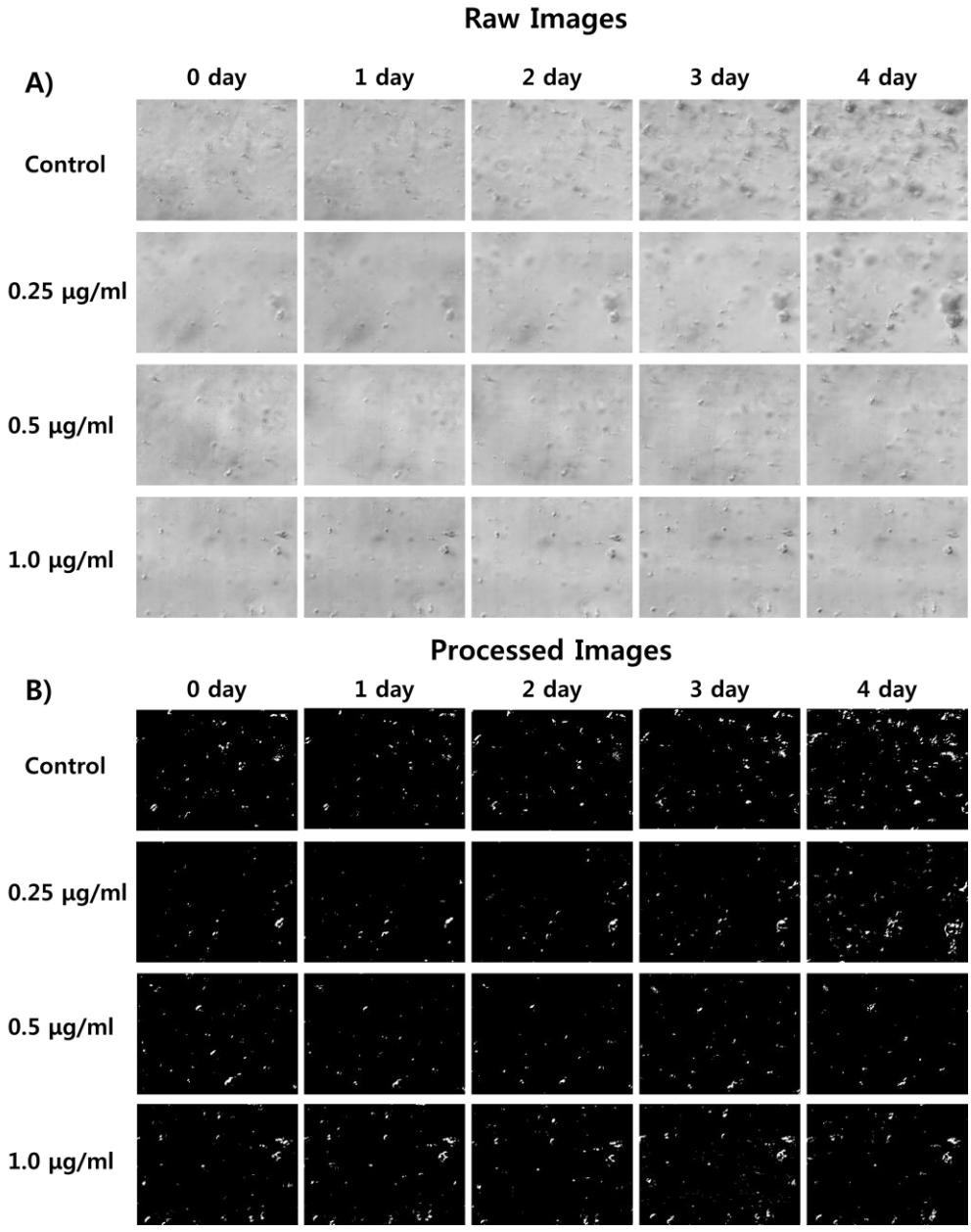

Figure 5.4 Time Lapse Images and Processed Images. A) Raw images of H37Rv in condition of rifampicin B) Processed images. In the resistant case, many colonies of

MTB formed and grew in the imaging area. After image processing, the white area represent the growing MTB colonies in the images. In the susceptible cases, there was no change of the MTB grown in the images.

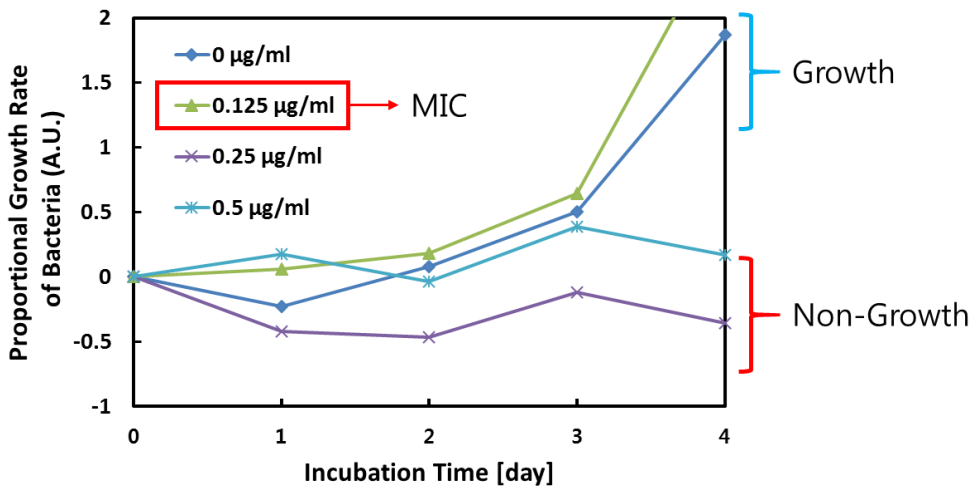

Figure 5.5 Quantification of growth dynamics in the resistant and susceptible cases. By measuring the grown areas of MTB in the images, the growth curve was plotted. In the resistant case, the area of MTB in the images were continuously increased and the areas showed on change in the susceptible case.

Rapid DSTs are needed for an urgent public health and diagnostics due to increasing patients and suspects of the MDR, XDR, and TDR globally. DAC system gives an opportunity for rapid DST by concept of microfluidic channel. To validate the DAC system for rapid DST, virulent standard strain of TB, H37Rv and clinical MDR and XDR strains were tested to determine the susceptibility of anti-tuberculosis drugs such as isoniazid, rifampicin, streptomycin, and ethambutol. A conventional DST, LJ culture DST was used as a composition target for quality control because the LJ culture DST are regarded as the golden standard. The MIC values of isoniazid, rifampicin, streptomycin, and ethambutol against H37Rv, MDR, and XDR that were determined by using the DAC system are shown in Table 5.1. From those MIC value, the susceptibility of H37Rv, MDR, and XDR against isoniazid, rifampicin, streptomycin, and ethambutol were decided by checking the MIC values were under the critical concentration or not. The images of all tested strains were taken at the same position every day for 5 days using a time-lapse method After image processing and graph plotting by using time-lapse data of every day for 5 days, the MIC value of 4 anti-tuberculosis drug against H37Rv were determined to be 0.05 μg/ml for isoniazid, 0.25 μg/ml for rifampicin, 2.0 μg/ml for streptomycin, and 5.0 μg/ml for ethambutol. From the MIC data, H37Rv strain was susceptible to isoniazid, rifampicin, streptomycin, and ethambutol and also LJ culture test gave the same results. In two of other tested strains, MDR and XDR patient strains were all

resistant from DAC system. The susceptibility results were verified using the gold standard LJ method. All susceptibility results for the DAC system were same with gold standard method's results. From these verified results, the DAC system reduced the DST time and generated accurate DST results for diagnosing the susceptible and resistant of anti-tuberculosis drugs.

Table 5.1 The DST results from the DAC system. H37Rv, MDR and XDR TB strains were tested with 4 primary TB drugs, isoniazid (INH), rifampicin (RFP), streptomycin (SM), and ethambutol (EMB). The testing concentrations were determined from the critical concentration of each drugs. After determination of MIC from the time lapse images, the value were examined by the break point and drug susceptibility was determined. A) MIC values of DST from DAC b) susceptibility determination using MIC data and critical concentrations of drugs

A

Sample#	H37Rv	MDR	XDR
INH	0.05	>0.2	>0.2
RFP	0.25	>2.0	>2.0
SM	2.0	>4.0	>4.0
EMB	5.0	>10.0	10.0

B

Sample#	H37Rv	MDR	XDR
INH	S	R	R
RFP	S	R	R
SM	R	R	R
EMB	S	R	R

5.2.4 Discussion

In this chapter, rapid DST platform based on single cell growth tracking of MTB in the agarose matrix is introduced. This DST method can be the fastest way of among the phenotype DST systems. To track the MTB growth under microscope, the immobilization of MTB with stable delivery of culture medium and drugs was required. Agarose has been proven as a bio-compatible material and also as a good material for diffusion of culture media, so has been selected for 3D culture. The immobilized TB cells in agarose were divided and the growth of MTB cells was observed under microscopy with time laps imaging. Considering its dividing time, drug susceptibility of TB could be determined in 3~4 days after 3~4 times cell dividing resulting in 10~20 time increase in cell volume. In our research, the growth of TB was detected and DST results were derived only in 4 days. 40X lens was used to observe the growth of TB. If a higher magnification lens was used (100x lens), the time of DST could be reduced to 2~3 days because the growth of TB could be detected more in detail.

The DAC system can have characteristics of both liquid and solid medium culture systems. In the liquid culture system, the growth of TB is accelerated due to the supplement, OADC. However, in the liquid culture system, single cell tracking is difficult resulting from that single cell cannot be immobilized to produce inevitable errors in detection of MTB cells. Therefore, we immobilized TB cells with agarose

without compromise of the growth rate in liquid media.

The MTB cells in the agarose matrix were from the pre-cultured colonies on the LJ medium. Recently, an automated liquid culture system, BD MGIT, has been used for culture of TB from patients' sputum. For a direct DST after MTB culture, the MTB positive sample from MGIT tube can be used. The DST cost of MGIT is known to relatively expensive. Considering high-throughput test with all drugs for TB (about 15 kinds of drugs), which is too expensive in the MGIT system. If the DAC DST system is integrated with the MGIT culture system, the DST from patients' sputum could be done in two or three weeks with very low cost resulting in 6~7 times faster than the conventional systems.

In this study, only 4 primary drugs were tested for MTB strains. The PMMA chip is easily expanded for DST with all the TB drugs. The all TB drug testing system in the DAC system could make it possible to prescribe the proper drugs for the TB patients in one week. That rapid and accurate DST will increase the cure rate of TB and help reduce the spread of resistant TB eventually.

5.3 Summary

In summary, the single cell growth tracking of MTB in the agarose matrix produced a rapid DST in 4 days. The agarose matrix provided 3 D culture environment which is suitable for TB culture and DST supplying culture media and drugs with the microscopic imaging method. The standard strain, H37Rv, MDR and XDR MTB strains were tested in this platform and resulted in comparable data with the conventional method. This DST methods could be used as a rapid DST method and help contribute to reduction of the global health problems related in MTB.

Chapter 6 Conclusions and Future Works

In this dissertation, a new method for reducing the time for drug susceptibility test was introduced. By single cell tracking of bacteria immobilized in agarose, the response of bacteria against drugs was determined faster than conventional methods. For validation of single cell tracking method, a microfluidic chip was designed and tested with standard strains. Bacteria are fixed in a thin agarose matrix, and different concentrations of antibiotics are supplied to the bacteria by diffusion. The growth of single bacterial cells is tracked by microscopy according to the incubation time, and the images are processed through our own image processing program to determine MIC values. The entire AST process takes 3–4 h, and it produces data that is comparable in accuracy to the conventional AST results of the CLSI.

For clinical application, the system requires covering all kinds of antibiotics used in clinics and high-throughput. A microfluidic agarose channel (MAC) chip integrated with 96 well plate was fabricated. During the testing of many kinds of antibiotics, morphological changes were found in Gram-negative strain in beta-

lactam antibiotic conditions. By observing the morphological changes with gold standard test, broth microdilution test, a new judgment criteria for AST was established from single-cell morphological analysis (SCMA). The SCMA with MAC chip could derive results satisfying the standard recommend by U.S. Food and Drug Administration.

For rapid drug susceptibility of *M. tuberculosis*, the chip should be sustainable for one week. The agarose matrix provided 3 D culture environment which is suitable for TB culture and DST supplying culture media and drugs with the microscopic imaging method. The standard strain, H37Rv, MDR and XDR MTB strains were tested in this platform and resulted in comparable data with the conventional method.

The direction of future works is focused on the direct drug susceptibility test from clinical sample such as blood and sputum. In case of AST, the isolation of bacteria from patients' sample consumes more time than AST itself. For ultimate rapid AST, the AST should be performed from blood sample. The critical hindrances of AST from blood sample are extremely low concentration and impurities in blood. To overcome the issues, a new test chip should detect the growth of small number of bacteria.

For DST, the test was started from the cultured strain in solid media. However, developing countries do not have resources to culture the TB from sputum and

cannot perform DST that requires bio safety level (BSL) 3 facility. Therefore, a new system can detect drug resistance from sputum called direct DST system is necessary. Also, for application in the region without electricity, the test system should be performed in low electricity such as solar cell. For low power usage, the optical detection method is not favorable and electrical sensor system is preferred. There are many studies that use electrical sensor for detecting bacterial growth. I will combine the electrical sensor with culture chip for determining drug susceptibility from sputum culture.

The rapid drug susceptibility test based on single cell tracking method will be used for fast and accurate drug treatment in clinical area. It will contribute to control the emergency of drug resistance strains.

Bibliography

[1] K. Bourzac, "Infectious disease: Beating the big three". *Nature* **507**, S4-S7, 2014.

[2] W. H. Organization, "Global tuberculosis report 2013". *World Health Organization*, 2013.

[3] N. R. Gandhi, P. Nunn, K. Dheda, H. S. Schaaf, M. Zignol, D. Van Soolingen, P. Jensen, J. Bayona, "Multidrug-resistant and extensively drug-resistant tuberculosis: a threat to global control of tuberculosis". *The Lancet* **375**, 1830-1843, 2010.

[4] Z. F. Udwadia, R. A. Amale, K. K. Ajbani, C. Rodrigues, "Totally Drug-Resistant Tuberculosis in India". *Clinical Infectious Diseases* **54**, 579-581, 2012.

[5] L. Heifets, G. Cangelosi, "Drug susceptibility testing of Mycobacterium tuberculosis: a neglected problem at the turn of the century State of the Art". *The International Journal of Tuberculosis and Lung Disease* **3**, 564-581, 1999.

[6] A. Cheng, M. Li, C. Chan, C. Chan, D. Lyon, R. Wise, J. Lee, "Evaluation of three culture media and their combinations for the isolation of Mycobacterium tuberculosis from pleural aspirates of patients with tuberculous pleurisy". *The Journal of tropical medicine and hygiene* **97**, 249-253, 1994.

[7] P. Bemer, F. Palicova, S. Rüsch-Gerdes, H. B. Drugeon, G. E. Pfyffer, "Multicenter Evaluation of Fully Automated BACTEC Mycobacteria Growth Indicator Tube 960 System for Susceptibility Testing of Mycobacterium tuberculosis". *Journal of clinical microbiology* **40**, 150-154, 2002.

[8] J. Choi, Y.-G. Jung, J. Kim, S. Kim, Y. Jung, H. Na, S. Kwon, "Rapid antibiotic susceptibility testing by tracking single cell growth in a microfluidic agarose channel system". *Lab on a Chip* **13**, 280-287,

2013.

[9] J. Chen, G. Z. Zou, X. L. Zhang, W. R. Jin, "Ultrasensitive electrochemical immunoassay based on counting single magnetic nanobead by a combination of nanobead amplification and enzyme amplification". *Electrochemistry Communications* **11**, 1457-1459, 2009.

[10] H. Cho, H.-Y. Kim, J. Y. Kang, T. S. Kim, "How the capillary burst microvalve works". *Journal of Colloid and Interface Science* **306**, 379-385, 2007.

[11] D. C. Duffy, J. C. McDonald, O. J. A. Schueller, G. M. Whitesides, "Rapid Prototyping of Microfluidic Systems in Poly(dimethylsiloxane)". *Analytical Chemistry* **70**, 4974-4984, 1998.

[12] M. A. Wikler, F. R. Cockerill, K. Bush, M. N. Dudley, G. M. Elipoulos, D. J. Hardy, D. W. Hecht, J. F. Hindler, J. B. Patel, M. Powell, J. D. Turnidge, M. P. Weinstein, B. L. Zimmer, M. J. Ferraro, J. M. Swenson, "Methods for dilution antimicrobial susceptibility tests for bacteria that grow aerobically: approved standard". **29**, 2009.

[13] H. A. Awad, M. Quinn Wickham, H. A. Leddy, J. M. Gimble, F. Guilak, "Chondrogenic differentiation of adipose-derived adult stem cells in agarose, alginate, and gelatin scaffolds". *Biomaterials* **25**, 3211-3222, 2004.

[14] L. B. Reller, M. Weinstein, J. H. Jorgensen, M. J. Ferraro, "Antimicrobial Susceptibility Testing: A Review of General Principles and Contemporary Practices". *Clinical Infectious Diseases* **49**, 1749-1755, 2009.

[15] V. Horák, "R factors of Escherichia coli strains causing urinary tract infections, their types of transfer factors and differences in their transmissibility toCitrobacter andSalmonella typhimurium recipient strains". *Folia microbiologica* **16**, 317-322, 1971.

[16] E. Southern, "Detection of specific sequences among DNA fragments

separated by gel electrophoresis". *Journal of Molecular Biology*, 98, 1975.

[17] N. Pernodet, M. Maaloum, B. Tinland, "Pore size of agarose gels by atomic force microscopy". *Electrophoresis* **18**, 55-58, 1997.

[18] S. Liang, J. Xu, L. Weng, H. Dai, X. Zhang, L. Zhang, "Protein diffusion in agarose hydrogel in situ measured by improved refractive index method". *Journal of Controlled Release* **115**, 189-196, 2006.

[19] W. Costerton, R. Veeh, M. Shirtliff, M. Pasmore, C. Post, G. Ehrlich, "The application of biofilm science to the study and control of chronic bacterial infections". *The Journal of Clinical Investigation* **112**, 1466-1477, 2003.

[20] S. Jin, Y. Yin, "Research on rapid detection of total bacteria in juice based on biomimetic pattern recognition and machine vision". *2010 3rd IEEE International Conference* **6**, 395-399, 2010.

[21] S. Pukatzki, R. H. Kessin, J. J. Mekalanos, "The human pathogen Pseudomonas aeruginosa utilizes conserved virulence pathways to infect the social amoeba Dictyostelium discoideum". *Proceedings of the National Academy of Sciences* **99**, 3159, 2002.

[22] P. S. Mead, L. Slutsker, V. Dietz, L. F. McCaig, J. S. Bresee, C. Shapiro, P. M. Griffin, R. V. Tauxe, "Food-related illness and death in the United States". *Emerging Infectious Diseases* **5**, 607, 1999.

[23] F. D. Lowy, "Staphylococcus aureus infections". *New England Journal of Medicine* **339**, 520-532, 1998.

[24] C. Watanakunakorn, J. S. Tan, J. P. Phair, "Some salient features of Staphylococcus aureus endocarditis". *The American journal of medicine* **54**, 473-481, 1973.

[25] J. Davies, D. Davies, "Origins and evolution of antibiotic resistance". *Microbiology and Molecular Biology Reviews* **74**, 417-433, 2010.

[26] P. C. Appelbaum, "Reduced glycopeptide susceptibility in methicillin-resistant Staphylococcus aureus (MRSA)". *International*

Journal of Antimicrobial Agents **30**, 398-408, 2007.

[27] H. H. Tuson, G. K. Auer, L. D. Renner, M. Hasebe, C. Tropini, M. Salick, W. C. Crone, A. Gopinathan, K. C. Huang, D. B. Weibel, "Measuring the stiffness of bacterial cells from growth rates in hydrogels of tunable elasticity". *Molecular Microbiology* **84**, 874-891, 2012.

[28] C. H. Chen, Y. Lu, M. L. Y. Sin, K. E. Mach, D. D. Zhang, V. Gau, J. C. Liao, P. K. Wong, "Antimicrobial susceptibility testing using high surface-to-volume ratio microchannels". *Analytical Chemistry* **82**, 1012-1019, 2010.

[29] D. L. Popham, K. D. Young, "Role of penicillin-binding proteins in bacterial cell morphogenesis". *Current Opinion in Microbiology* **6**, 594-599, 2003.

[30] W. Margolin, "Sculpting the bacterial cell". *Current Biology* **19**, R812-R822, 2009.

[31] D. F. Stickle, D. A. Lauffenburger, S. H. Zigmond, "Measurement of chemoattractant concentration profiles and diffusion coefficient in agarose". *Journal of immunological methods* **70**, 65-74, 1984.

[32] S. Liang, J. Xu, L. Weng, H. Dai, X. Zhang, L. Zhang, "Protein diffusion in agarose hydrogel in situ measured by improved refractive index method". *J Control Release* **115**, 189-196, 2006.

[33] J. H. Humphrey, J. W. Lightbown, "A General Theory for Plate Assay of Antibiotics with some Practical Applications". *Journal of general microbiology* **7**, 129-143, 1952.

[34] P. Dalgaard, T. Ross, L. Kamperman, K. Neumeyer, T. A. McMeekin, "Estimation of bacterial growth rates from turbidimetric and viable count data". *Int J Food Microbiol* **23**, 391-404, 1994.

[35] J. Choi, J. Yoo, M. Lee, E.-G. Kim, J. S. Lee, S. Lee, S. Joo, S. H. Song, E.-C. Kim, J. C. Lee, H. C. Kim, Y.-G. Jung, S. Kwon, "A rapid antimicrobial susceptibility test based on single-cell morphological

analysis". *Science Translational Medicine* **6**, 267ra174, 2014.

[36] H. W. Boucher, G. H. Talbot, J. S. Bradley, J. E. Edwards, D. Gilbert, L. B. Rice, M. Scheld, B. Spellberg, J. Bartlett, "Bad bugs, no drugs: no ESKAPE! An update from the Infectious Diseases Society of America". *Clinical Infectious Diseases* **48**, 1-12, 2009.

[37] L. B. Rice, "Federal funding for the study of antimicrobial resistance in nosocomial pathogens: no ESKAPE". *Journal of Infectious Diseases* **197**, 1079-1081, 2008.

[38] I. Peitz, R. van Leeuwen, "Single-cell bacteria growth monitoring by automated DEP-facilitated image analysis". *Lab on a Chip* **10**, 2944-2951, 2010.

[39] Y. Lu, J. Gao, D. D. Zhang, V. Gau, J. C. Liao, P. K. Wong, "Single cell antimicrobial susceptibility testing by confined microchannels and electrokinetic loading". *Anal Chem* **85**, 3971-3976, 2013.

[40] C. S. Price, S. E. Kon, S. Metzger, "Rapid antibiotic susceptibility phenotypic characterization of Staphylococcus aureus using automated microscopy of small numbers of cells". *Journal of Microbiological Methods* **98**, 50-58, 2014.

[41] F. R. Cockerill, M. A. Wikler, K. Bush, D. M.N., G. M. Elipoulos, D. J. Hardy, D. W. Hecht, J. A. Hindler, J. B. Patel, M. Powell, R. B. Thomson, J. D. Turnidge, M. P. Weinstein, B. L. Zimmer, M. J. Ferraro, J. M. Swenson, "Performance Standards for Antimicrobial Susceptibility Testing of Anaerobic Bacteria: Informational Supplement". **31**, 2011.

[42] F. D. Administration, "Class II special controls guidance document: antimicrobial susceptibility test (AST) systems; guidance for industry and FDA". *US Department of Health and Human Services, Food and Drug Administration, Washington, DC*, 1-48, 2009.

[43] G. V. Doern, R. Vautour, M. Gaudet, B. Levy, "Clinical impact of rapid in vitro susceptibility testing and bacterial identification".

Journal of clinical microbiology **32**, 1757-1762, 1994.

[44] J. Buijs, A. S. M. Dofferhoff, J. W. Mouton, J. H. T. Wagenvoort, J. W. M. Van Der Meer, "Concentration-dependency of β-lactam-induced filament formation in Gram-negative bacteria". *Clinical Microbiology and Infection* **14**, 344-349, 2008.

[45] N. J. Cira, J. Y. Ho, M. E. Dueck, D. B. Weibel, "A self-loading microfluidic device for determining the minimum inhibitory concentration of antibiotics". *Lab Chip* **12**, 1052-1059, 2012.

[46] M. A. C. Broeren, Y. Maas, E. Retera, N. L. A. Arents, "Antimicrobial susceptibility testing in 90 min by bacterial cell count monitoring". *Clinical Microbiology and Infection* **19**, 286-291, 2013.

[47] E. Carbonnelle, C. Mesquita, E. Bille, N. Day, B. Dauphin, J.-L. Beretti, A. Ferroni, L. Gutmann, X. Nassif, "MALDI-TOF mass spectrometry tools for bacterial identification in clinical microbiology laboratory". *Clinical biochemistry* **44**, 104-109, 2011.

[48] N. Fatin-Rouge, K. Starchev, J. Buffle, "Size effects on diffusion processes within agarose gels". *Biophysical Journal* **86**, 2710-2719, 2004.

국문 초록

본 논문은 결핵균의 항생제 감수성 검사를 신속하게 할 수 있는 원리와 시스템을 제시한다. 단일 세포를 아가로즈 안에 가둔 뒤에 배양액과 약제를 확산에 의한 방법으로 공급하는 시스템을 개발하였다. 단일 세포의 약물에 대한 반응을 현미경으로 관찰한 뒤에 그 변화를 이미지 프로세싱을 통해 정량화하여서 약제 감수성 검사를 수행하였다. 먼저 일반 균주의 경우 3~4 시간에 표준 방법과 잘 대응하는 결과를 도출하였다. 다양한 약제와 여러 균주의 항생제 감수성 검사를 위해서 단일세포 형태 분석 방법을 고안하여 FDA 기준에 적합한 결과를 도출하였다. 최종적으로 결핵균을 배양할 수 있는 시스템을 개발하였고 단일 세포 관측을 통해서 일주일 안에 결핵균의 항생제 감수성 검사를 할 수 있는 시스템을 개발하였다. 이 기술이 현재 전세계적으로 문제가 되고 있는 결핵과 항생제 내성 문제를 해결하는데 사용될 수 있음을 보여 주었다.

주요어 : 결핵, 항생제 내성, 단일 세포 추적, 아가로즈, 약제 감수성 검사

학번 : 2011-30261p